Organometallics **1999,** *18,* 5447−5459

Half-Sandwich Group 4 Metal Siloxy and Silsesquioxane Complexes: Soluble Model Systems for Silica-Grafted Olefin Polymerization Catalysts

Robbert Duchateau,*,† Ulrich Cremer,† Roelant J. Harmsen,† Said I. Mohamud,†
Hendrikus C. L. Abbenhuis,† Rutger A. van Santen,† Auke Meetsma,‡
Sven K.-H. Thiele,§ Maurits F. H. van Tol,§ and Mirko Kranenburg§

Schuit Institute of Catalysis, Eindhoven University of Technology, P.O. Box 513,
5600 MB Eindhoven, The Netherlands, University of Groningen, Nijenborgh 4,
9747 AG Groningen, The Netherlands, and DSM Research BV, P.O. Box 18,
6160 MD Geleen, The Netherlands

Received June 10, 1999

The cuboctameric hydroxysilsesquioxane ($(c\text{-}C_5H_9)_7Si_8O_{12}(OH)$ (**2**), obtained after hydrolysis of $(c\text{-}C_5H_9)_7Si_8O_{12}Cl$ (**1**), and triphenylsilanol have been applied as model supports for silica-grafted olefin polymerization catalysts. The ligands were introduced on group 4 metals by either chloride metathesis or protonolysis. Treatment of $Cp''MCl_3$ (M = Ti, Zr; Cp″ = 1,3-$C_5H_3(SiMe_3)_2$) with silsesquioxane and siloxylithium or -thallium salts, $[(c\text{-}C_5H_9)_7Si_8O_{13}]M'$ (M′ = Tl (**3**), Li (**4**), Li·TMEDA (**5**)) or Ph_3SiOTl gave either the dichloride complexes $Cp''[(c\text{-}C_5H_9)_7Si_8O_{13}]MCl_2$ (M = Ti (**6a**), Zr (**7a**)) and $Cp''[Ph_3SiO]TiCl_2$ (**8a**) or the monochloride species $Cp''[(c\text{-}C_5H_9)_7Si_8O_{13}]_2MCl$ (M = Ti (**6b**), Zr (**7b**)) and $Cp''[Ph_3SiO]_2MCl$ (M = Ti (**8b**), Zr (**9**)). Similarly, protonolysis of $Cp''MR_3$ with the silanols **2** and Ph_3SiOH yielded the corresponding silsesquioxane bis(alkyl) complexes $Cp''[(c\text{-}C_5H_9)_7Si_8O_{13}]TiR_2$ (R = CH_2Ph (**10a**), Me (**10b**)) and triphenylsiloxy bis(alkyl) compounds $Cp''[Ph_3SiO]MR_2$ (M = Ti, R = CH_2Ph (**11a**), Me (**11b**); M = Zr, R = CH_2Ph (**12a**)) and the monobenzyl complex $Cp''[Ph_3SiO]_2ZrCH_2Ph$ (**12b**). When activated with MAO, not only the dichloride complexes (**6a**, **7a**, **8a**) but also the monochlorides (**6b**, **7b**, **8b**, **9**) yield active ethylene polymerization catalysts. The observation that even complexes containing a tridentate silsesquioxane ligand, $[(c\text{-}C_5H_9)_7Si_8O_{12}]MCp''$ (M = Ti (**13**), Zr (**14**)), form active ethylene polymerization catalysts when activated with MAO indicates that silsesquioxane and siloxy ligands are easily substituted by MAO. The silsesquioxane and siloxy bis(alkyl) complexes (**10**, **11**, **12a**) form active olefin polymerization catalysts when activated with $B(C_6F_5)_3$, which leaves the M−O bond unaffected. Although the different cone angles of $(c\text{-}C_5H_9)_7Si_8O_{13}$ (155°) and Ph_3SiO (132°) suggest otherwise, the effective steric congestion around the metal center of $(c\text{-}C_5H_9)_7Si_8O_{13}$- and Ph_3SiO-stabilized complexes was found to be reasonably comparable. The electronic differences between $(c\text{-}C_5H_9)_7Si_8O_{12}(OH)$ (**2**) and Ph_3SiOH are more pronounced. pK_a measurements and DFT calculations indicate that **2** is notably more Brønsted acidic and electron withdrawing than Ph_3SiOH.

Introduction

Heterogenization of well-defined homogeneous olefin polymerization catalysts offers opportunities to combine the advantages of both supported and homogeneous catalysts.[1] In the ideal case, morphology control by replication leads to uniform polymer particles with narrow particle size distribution and high bulk density,[2] whereas the single-site nature of the catalyst provides polymers with narrow molecular weight distributions. Additionally, immobilization of the catalyst can reduce the formation of dormant sites, which, in principle, makes it possible to decrease the necessary amount of cocatalyst.[3a,h−j] The most common method to immobilize

---

* To whom correspondence should be addressed. E-mail: R.Duchateau@tue.nl. Fax: +31-40-2455054.
† Eindhoven University of Technology.
‡ University of Groningen.
§ DSM Research BV.

(1) (a) Zakharov, V. A.; Yermakov, Y. I. *Catal. Rev.-Sci. Eng.* **1979**, *19*, 67. (b) Collette, J. W.; Tullock, C. W. U.S. Pat. Appl. 4,298,722, 1981 (c) Gahleitner, M.; Ledwinka, H.; Hafner, N.; Neissl, W. *Proceedings of Sixth International Business Forum on Specialty Polyolefins, SPO '96*, **1996**, p 283. (d) Marsden, C. E. *Plast., Rubber Compos. Process. Appl.* **1994**, *21*, 193. (e) *Catalytic Polymerization of Olefins, Studies in Surface Science and Catalysis*; Keii, T., Soga, K., Eds.; Elsevier: New York, 1986. (f) *Transition Metals and Organometallics as Catalysts for Olefin Polymerization*; Kaminsky, W., Sinn, H., Eds.; Springer-Verlag: New York, 1988. (g) Olabisi, O.; Atiqulla, M.; Kaminsky, W. *Makromol. Chem. Phys.* **1997**, *C37*(3), 519 and references therein.

10.1021/om9904495 CCC: $18.00 © 1999 American Chemical Society
Publication on Web 11/19/1999

homogeneous olefin polymerization catalysts consists of physisorption of metallocenes on a support that is pretreated with methylalumoxane (MAO) or other cocatalysts.[1e−g,3] Whereas this method results in heterogeneous catalysts, leaching remains one of the major problems. Improvement of this and alternative immobilization techniques, such as catalyst tethering[4] and grafting,[1a−d,5] remains therefore a topic of great importance.

To get more insight, at a molecular level, into processes taking place at silica surfaces and to improve the immobilization methodologies, suitable homogeneous model systems for silica surface silanol sites are of great importance. The major advantage of such homogeneous model systems is that their structural properties and reactivity can be studied in detail using a wide range of powerful techniques such as multinuclear solution NMR spectroscopy. Several siloxy- and silsesquioxane-stabilized group 4 metal complexes have been used as models for silica-grafted systems.[6,7] Recently, the importance of homogeneous model systems for heterogeneous catalysis has clearly been demonstrated by the development of titanasilsesquioxane complexes $[R_7Si_7O_{12}]TiX$ ($R = c\text{-}C_5H_9$, $c\text{-}C_6H_{11}$; X = alkyl, alkoxide, amido, cyclopentadienyl),[7g,h,8] which are active olefin epoxidation catalysts and mimic titanium sites in heterogeneous epoxidation catalysts such as TS-1 and titanium grafted on MCM-41.[9]

As part of a project on immobilization of homogeneous olefin polymerization catalysts, we were interested in modeling grafting of group 4 metal complexes onto partly dehydroxylated silica. With regard to olefin polymerization, silica-grafted species of the type $[SiO_2]{-}O{-}M(Cp)X_2$ (X = chloride, alkyl), containing two chloride or alkyl substituents, are of interest.[1g,10] Preparation of such heterogeneous catalysts can be simplified considerably using synthetic strategies developed for homogeneous model complexes. Hence, we were looking for simple yet realistic models for isolated silanol functionalities as found in partially dehydroxylated silica.

Here we report the use of triphenylsilanol, Ph_3SiOH, and the cuboctameric hydroxysilsesquioxane $(c\text{-}C_5H_9)_7Si_8O_{12}(OH)$ as homogeneous supports to mimic grafting of group 4 metal half-sandwich complexes onto partly dehydroxylated silica. The olefin polymerization activity of the metallasiloxy and metallasilsesquioxane complexes is studied, as well as the stability of the complexes against leaching. Finally, to get an insight into the differences between Ph_3SiOH and $(c\text{-}C_5H_9)_7Si_8O_{12}(OH)$ and to assess the suitability of these ligands as models for silica surface silanol sites, the steric and electronic differences between Ph_3SiOH and $(c\text{-}C_5H_9)_7Si_8O_{12}(OH)$ are investigated. Parts of this work have been communicated.[11]

Results and Discussion

Cuboctameric Hydroxysilsesquioxane and Anionic Derivatives. Recently, we reported the synthesis of the hydroxysilsesquioxane $(c\text{-}C_5H_9)_7Si_8O_{12}(OH)$.[11] Treating $(c\text{-}C_5H_9)_7Si_7O_9(OH)_3$ with 1 equiv of $SiCl_4$ in the presence of NEt_3 yielded the corner-capped chlorosilsesquioxane $(c\text{-}C_5H_9)_7Si_8O_{12}Cl$ (**1**; eq 1),[12] which, after subsequent hydrolysis in a mixture of THF and water (2:1), afforded the monosilanol $(c\text{-}C_5H_9)_7Si_8O_{12}(OH)$ (**2**; eq 1) as a white microcrystalline material. The hydrolysis is surprisingly slow, and 2 days of refluxing is required to complete the reaction.

Hydroxysilsesquioxane **2** is an interesting homogeneous model system for isolated silanol sites in partially dehydroxylated silica. Its high symmetry (C_{3v}) significantly facilitates NMR studies, whereas the cubic silsesquioxane framework of **2** is stable toward degradation by strong nucleophilic reagents.[13] Like all silsesquioxane silanols, compound **2** reacts cleanly with 1 equiv of TlOEt in toluene to afford thin white needles

---

[2] For example see: Hungenberg, K. H.; Kerth, J.; Langhauser, F.; Marczinke, B.; Schlund, R. In *Ziegler Catalysts*; Fink, G., Mülhaupt, R., Brintzinger, H. H., Eds.; Springer-Verlag: New York, 1995; Chapter 20.

[3] (a) Chien, J. C. W.; He, D. *J. Polym. Sci., Part A: Polym. Chem.* **1991**, 1603. (b) Van Looveren, L. K.; Geysen, D. F. M. C.; Vercruysse, K. A. L.; Wouters, B. H. J.; Grobet, P. J.; Jacobs, P. A. *Angew. Chem.* **1998**, *110*, 540. (c) Kaminsky, W.; Renner, F. *Makromol. Chem., Rapid Commun.* **1993**, *14*, 239. (d) Ko, Y. S.; Han, T. K.; Park, J. W.; Woo, S. I. *Macromol. Rapid Commun.* **1996**, *17*, 749. (e) Kaminaka, M.; Soga, K. *Makromol. Chem., Rapid Commun.* **1991**, *12*, 367. (f) Soga, K.; Kaminsky, W. *Makromol. Chem., Rapid Commun.* **1992**, *13*, 221. (g) Soga, K.; Kaminsky, W. *Makromol. Chem.* **1993**, *194*, 1745. (h) Chien, J. C. W. *Top. Catal.* **1999**, *7*, 23 and references therein. (i) Welborn, H. C. Jr. U.S Pat. Appl. 4,897,455, 1990. (j) Canich, J.-A. M.; Licciardi, G. P. U.S. Pat. Appl. 5,057,475, 1991.

[4] (a) Iiskola, E. I.; Timonen, S.; Pakkanen, T. T.; Härkki, O.; Lehmus, P.; Seppälä, J. V. *Macromolecules* **1997**, *30*, 2853. (b) Arai, T.; Ban, H. T.; Uozumi, T.; Soga, K. *J. Polym. Sci., Part A: Polym. Chem.* **1998**, *36*, 421. (c) Arai, T.; Ban, H. T.; Uozumi, T.; Soga, K. *Macromol. Chem. Phys.* **1997**, *198*, 237.

[5] (a) Ballard, D. G. H. *Adv. Catal.* **1973**, *23*, 263. (b) Schwartz, J.; Ward, M. D. *J. Mol. Catal.* **1980**, *8*, 465. (c) King, S. A.; Schwartz, J. *Inorg. Chem.* **1991**, *30*, 3771. (d) Scott, S. L.; Basset, J.-M.; Niccolai, G. P.; Santini, C. C.; Candy, J.-P.; Lecuyer, C.; Quignard, F.; Choplin, A. *New J. Chem.* **1994**, *18*, 115. (e) Vidal, V.; Théolier, A.; Thivolle-Cazat, J.; Basset, J.-M.; Corker, J. *J. Am. Chem. Soc.* **1996**, *118*, 4595. (f) Quignard, F.; Lécuyer, C.; Choplin, A.; Basset, J.-M. *J. Chem. Soc., Dalton Trans.* **1994**, 1153. (g) Ajjou, J. A.; Scott, S. *Organometallics* **1997**, *16*, 86. (h) Bade, O. M.; Blom, R.; Ystenes, M. *Organometallics* **1998**, *17*, 2524. (i) Theopold, K. H. *Eur. J. Inorg. Chem.* **1998**, 15 and references therein.

[6] For example see: (a) Bennet, J. L.; Wolczanski, P. T. *J. Am. Chem. Soc.* **1997**, *119*, 10696 and references therein. (b) Murugavel, R.; Chandrasekhar, V.; Roesky, H. W. *Acc. Chem. Res.* **1996**, *29*, 183. (c) Winkhofer, N.; Voigt, A.; Dorn, H.; Roesky, H. W.; Steiner, A.; Stalke, D.; Reller, A. *Angew. Chem.* **1994**, *106*, 1414. (d) Voigt, A.; Murugavel, R.; Montero, M. L.; Wessel, H.; Liu, F.-Q.; Roesky, H. W.; Usón, I.; Albers, T.; Parisini, E. *Angew. Chem.* **1997**, *109*, 1020. (e) Murugavel, R.; Voigt, A.; Walawalkar, M. G.; Roesky, H. W. *Chem. Rev.* **1996**, *96*, 2205.

[7] (a) Feher, F. J.; Blanski, R. L. *J. Chem. Soc., Chem. Commun.* **1990**, 1614. (b) Feher, F. J.; Blanski, R. L. *J. Am. Chem. Soc.* **1992**, *114*, 5886. (c) Liu, J.-C. *Chem. Commun.* **1996**, 1109. (d) Feher, F. J.; Blanski, R. L. *Makromol. Chem., Macromol. Symp.* **1993**, *66*, 95. (e) Feher, F. J.; Tajima, T. L. *J. Am. Chem. Soc.* **1994**, *116*, 2145. (f) Feher, F. J.; Walzer, J. F. *Inorg. Chem.* **1991**, *30*, 1689. (g) Crocker, M.; Herold, R. H. M.; Orpen, A. G. *Chem. Commun.* **1997**, 2411. (h) Krijnen, S.; Abbenhuis, H. C. L.; Hanssen, R. W. J. M.; van Hooff, J. H. C.; van Santen, R. A. *Angew. Chem., Int. Ed.* **1998**, *37*, 356. (i) Duchateau, R. Abbenhuis, H. C. L.; van Santen, R. A.; Meetsma, A.; Thiele, S. K.-H.; van Tol, M. F. H. *Organometallics* **1998**, *17*, 5663.

[8] (a) Abbenhuis, H. C. L.; Krijnen, S.; van Santen, R. A. *Chem. Commun.* **1997**, 331. (b) Crocker, M.; Herold, R. H. M. PCT Pat. Appl., WO97/24344. (c) Maschmeyer, T.; Klunduk, M. C.; Martin, C. M.; Shephard, D. S.; Thomas, J. M.; Johnson, B. F. G. *Chem. Commun.* **1997**, 1847.

[9] Corma, A.; Esteve, P.; Matínez, A.; Valencia, S. *J. Catal.* **1995**, *152*, 18 and references therein.

[10] For example see: (a) Park, J. R.; Shiono, T.; Soga, K. *Macromolecules* **1992**, *25*, 521. (b) Soga, K.; Lee, D. H. *Makromol. Chem.* **1992**, *193*, 1687. (c) Soga, K.; Koide, R.; Uozumi, T. *Makromol. Chem., Rapid Commun.* **1993**, *14*, 511. (d) Kratochvila, J.; Shiono, T.; Soga, K. *Makromol. Chem., Rapid Commun.* **1993**, *14*, 85. (e) Uozumi, T.; Toneri, T.; Soga, K. *Macromol. Rapid Commun.* **1997**, *18*, 9. (f) Xu, J.; Zhao, J.; Fan, Z.; Feng, L. *Macromol. Rapid Commun.* **1997**, *18*, 875. (g) Malinge, J. *Proceedings of Seventh International Business Forum on Specialty Polyolefins, SPO '97*; **1997**, p 123.

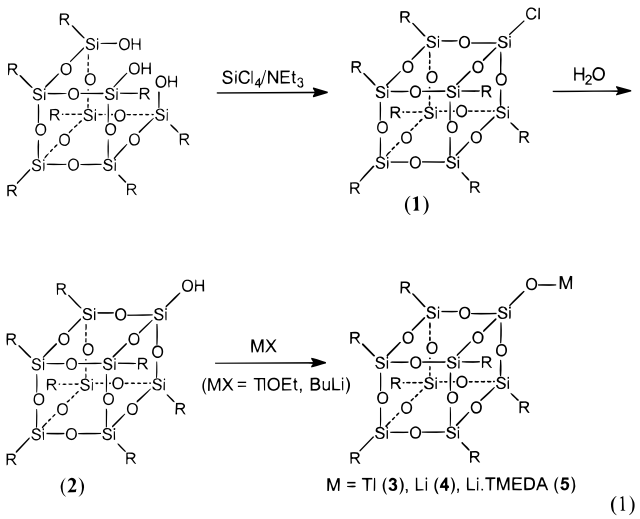

(1)

of the corresponding thallium salt $[(c\text{-}C_5H_9)_7Si_8O_{13}]Tl$ (**3**; eq 1) after crystallization from hexane. In accordance with the structurally characterized $\{[(c\text{-}C_6H_{11})_7Si_7O_9\text{-}(OSiMe_3)_2O]Tl\}_2$,[13b] the thallium silsesquioxane **3** is probably also dimeric. Similarly, deprotonation of **2** by an equimolar amount of *n*-BuLi in hexane solution selectively affords $\{[(c\text{-}C_5H_9)_7Si_8O_{13}]Li\}_n$ (**4**; eq 1). The extremely high hexane solubility of **4** suggests an oligomeric structure in apolar solvents. Treatment of **4** with TMEDA results in splitting of this oligomeric structure and gives the corresponding Lewis base adduct $[(c\text{-}C_5H_9)_7Si_8O_{13}]Li\cdot TMEDA$ (**5**; eq 1), which crystallizes as thin needles from hexane.

In $CDCl_3$, all cuboctameric silsesquioxanes described above display simple yet particularly informative ^{13}C and ^{29}Si NMR spectra showing well-resolved sets of *C*H-methine and Si resonances, consistent with the C_{3v} symmetry of the silsesquioxane ligand. Not unexpectedly, the ^1H NMR spectra are much less informative, due to the large number of similar CH_2 and CH protons present.

Half-Sandwich Group 4 Metal Chloride Silsesquioxane and Triphenylsiloxy Complexes. We first investigated halogen displacement routes to mono(silsesquioxane) and mono(triphenylsiloxy) chloride complexes $Cp''[(c\text{-}C_5H_9)_7Si_8O_{13}]MCl_2$ and $Cp''[Ph_3SiO]MCl_2$ ($Cp'' = 1,3\text{-}C_5H_3(SiMe_3)_2$), respectively.[14] The reaction of $Cp''TiCl_3$ with an equimolar amount of $[(c\text{-}C_5H_9)_7\text{-}Si_8O_{13}]Li$ (**4**) in hexane provides $Cp''[(c\text{-}C_5H_9)_7Si_8O_{13}]\text{-}TiCl_2$ (**6a**) as a bright yellow microcrystalline material after repeated recrystallization from hexane (Scheme 1). Independent of the silsesquioxane salt (**3**−**5**), solvent (hexane, toluene, ether, THF), and reaction temperature (−30 °C to reflux) used, small amounts (~10%) of $Cp''\text{-}[(c\text{-}C_5H_9)_7Si_8O_{13}]_2TiCl$ (**6b**) were also formed. Compound **6b** can directly be synthesized by salt metathesis of $Cp''TiCl_3$ with 2 equiv of **4** in hexane (Scheme 1). Despite its high solubility in organic solvents, which prevents crystallization, the high selectivity of this reaction allows isolation of analytically pure **6b** as lemon yellow foam after evaporation of the solvent.

Chloride substitution of $Cp''ZrCl_3$ with 1 equiv of **3** is less selective than for titanium and yields a 2:1 mixture of $Cp''[(c\text{-}C_5H_9)_7Si_8O_{13}]ZrCl_2$ (**7a**) and $Cp''[(c\text{-}C_5H_9)_7Si_8O_{13}]_2ZrCl$ (**7b**; Scheme 1). As for titanium, attempts to improve the selectivity of the reaction by varying the reaction conditions or silsesquioxane reagents failed. The similar solubilities of **7a** and **7b** prevented their separation, and as a result, complex **7a** could not be purified. On the other hand, analytically pure **7b** can be obtained by reacting $Cp''ZrCl_3$ with 2 equiv of **3** in toluene (Scheme 1). Attempts to substitute the last chloride in the bis(silsesquioxane) complexes **6b** and **7b** with another $[(c\text{-}C_5H_9)_7Si_8O_{13}]$ group failed, exclusively yielding ill-defined product mixtures. Probably steric reasons prevent clean substitution of the final chloride in these complexes.

The selectivity of the reactions of $Cp''MCl_3$ (M = Ti, Zr) with Ph_3SiOTl is similar to that observed with the silsesquioxane salts **3**−**5**. For example, the reaction of $Cp''TiCl_3$ with Ph_3SiOTl provides analytically pure $Cp''\text{-}[Ph_3SiO]TiCl_2$ (**8a**; Scheme 1) after repeated recrystallization from hexane to remove small amounts of $Cp''TiCl_3$ and $Cp''[Ph_3SiO]_2TiCl$ (**8b**). On the other hand, the equimolar reaction between Ph_3SiOTl and $Cp''ZrCl_3$ yields a 1:1 mixture of the bis(siloxy) complex $Cp''[Ph_3\text{-}SiO]_2ZrCl$ (**9**) and starting material, $Cp''ZrCl_3$, indicating that for zirconium the formation of the bis(siloxy) complex is clearly favored. Like **6b**/**7b**, the bis(triphenylsiloxy)titanium and -zirconium compounds $Cp''[Ph_3\text{-}SiO]_2MCl$ (M = Ti (**8b**), Zr (**9**)) are selectively formed by treatment of $Cp''MCl_3$ with 2 equiv of Ph_3SiOTl in toluene (Scheme 1). Attempts to substitute the final chloride in **8b** and **9** invariably failed.

The NMR data of the half-sandwich titanium and zirconium silsesquioxane complexes correspond well with each other. For example, the $^{13}C\{^1H\}$ NMR spectra of the mono(silsesquioxane) complexes $Cp''[(c\text{-}C_5H_9)_7\text{-}Si_8O_{13}]MCl_2$ (M = Ti (**6a**), Zr (**7a**)) display a single resonance for all seven methine (*C*H) carbons. In contrast, the $^{13}C\{^1H\}$ NMR spectra of the bis(silsesquioxane) complexes $Cp''[(c\text{-}C_5H_9)_7Si_8O_{13}]_2MCl$ (M = Ti (**6b**), Zr (**7b**)) show a well-resolved set of methine *C*H resonances (1:3:3 ratio), in agreement with the C_{3v} symmetry of the silsesquioxane ligand. ^{29}Si NMR spectroscopy proves to be a very useful tool for the characterization of silsesquioxane complexes, as the differences in chemical shift are large enough to distinguish between very similar complexes such as **6** and **7**, and the integrated relative intensities are in good agreement with the expected stoichiometries. For the metallasilsesquioxane complexes **6** and **7**, the ^{29}Si NMR spectra display four resonances in a 2:3:4:1 ratio for **6a**/**7a** and a 1:3:4:1 ratio for **6b**/**7b**, respectively: the Cp−*Si*Me$_3$ resonances are typically found around δ −7 ppm. The alkyl-substituted silsesquioxane silicon atoms, $(O)_3SiC_5H_9$, show two resonances in a 3:4 ratio (δ −65 and −68 ppm). Three of the seven silicon atoms, probably the ortho Si, are clearly distinct from the other

---

[11] Duchateau, R.; Abbenhuis, H. C. L.; van Santen, R. A.; Thiele, S. K.-H.; van Tol, M. F. H. *Organometallics* **1998**, *17*, 5222.

[12] Feher, F. J.; Weller, K. J.; Schwab, J. J. *Organometallics* **1995**, *14*, 2009.

[13] Several silsesquioxanes have found to be sensitive to nucleophilic attack. For example see: (a) Feher, F. J.; Budzichowski, T. A.; Rahimian, K.; Ziller, J. W. *J. Am. Chem. Soc.* **1992**, *114*, 3859. (b) Feher, F. J.; Rahimian, K.; Budzichowski, T. A.; Ziller, J. W. *Organometallics* **1995**, *14*, 3920. (c) Day, V. W.; Klemperer, W. G.; Mainz, V. V.; Millar, D. M. *J. Am. Chem. Soc.* **1985**, *107*, 8262.

[14] Introduction of bulky trimethylsilyl substituents on the cyclopentadienyl ligands significantly improved the selectivity of the reactions.

Scheme 1

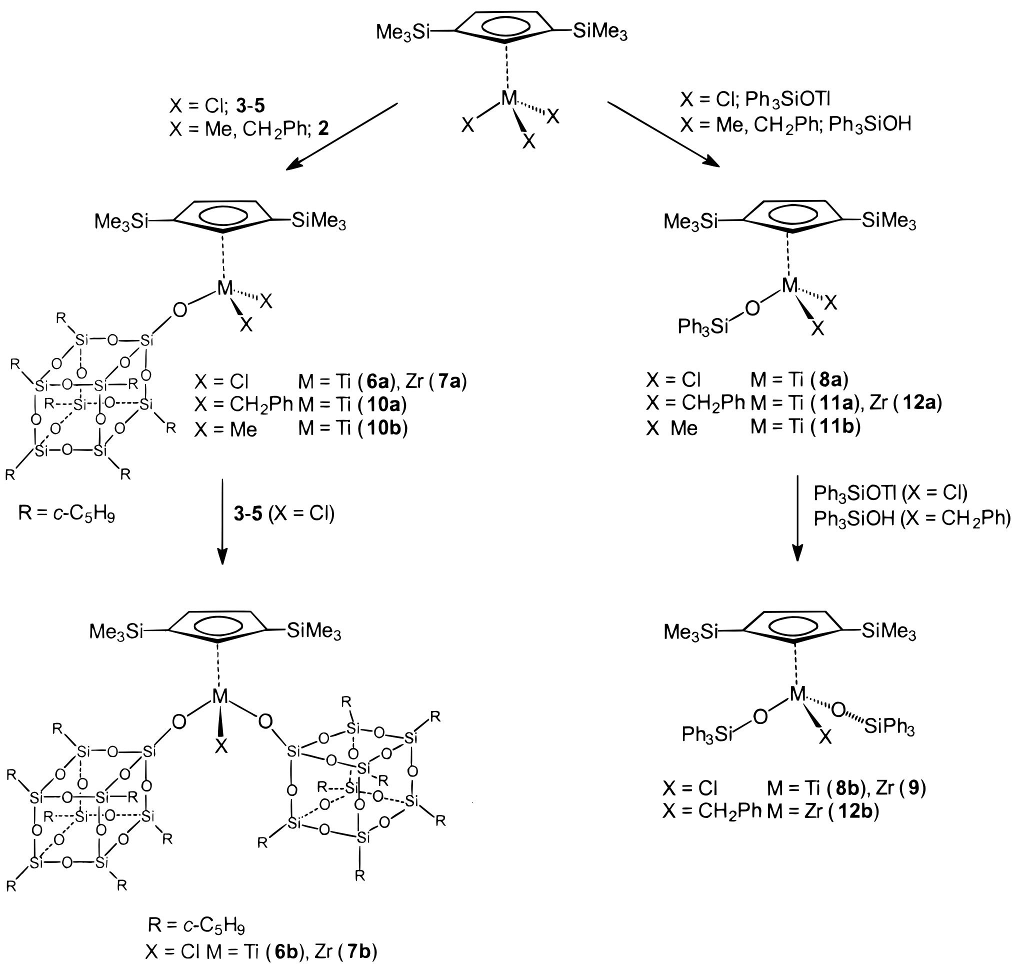

four, resulting in two resonances with observed relative intensities of 3:4. Finally, the ipso Si atom resonances appear around δ −110 ppm, characteristic for silicon surrounded by four oxygen atoms. For the corresponding triphenylsiloxy complexes **8** and **9** the ^{29}Si NMR spectra show two resonances in a 2:1 (**8a**, δ −6.3, −9.2 ppm) or 1:1 (**8b**, δ −7.3, −12.6 ppm; **9**, δ −8.5, −16.5 ppm) ratio for the Cp−*Si*Me$_3$ and Ph$_3$*Si*O silicon atoms, respectively.

X-ray Structure Determination of Cp″[Ph$_3$SiO]$_2$ZrCl (9). The poor crystallinity of the silsesquioxane complexes **6** and **7** prevented their single-crystal structure determinations.[15] The crystallinity of the corresponding triphenylsiloxy complexes **8** and **9** is much better, and slow crystallization of a saturated hexane solution at room temperature afforded Cp″[Ph$_3$SiO]$_2$ZrCl (**9**) as large colorless needles suitable for an X-ray diffraction study. A perspective view of the molecular structure of **9** is shown in Figure 1. Crystal data are collected in Table 1. Conformational disorder was observed for the two cyclopentadienyl trimethylsilyl substituents. One of the two conformations of both SiMe$_3$ substituents is shown. The structure consists of a three-legged piano-stool configuration in which the tetrahedrally surrounded zirconium atom is bonded to two siloxy groups, one chloride and one cyclopentadienyl ligand. The Zr−O bond distances (Zr−O(1) = 1.921(4) Å; Zr−O(2) = 1.929(5) Å) in **9** are short compared to those in zirconasilsesquioxane complexes [(c-C$_6$H$_{11}$)$_7$-

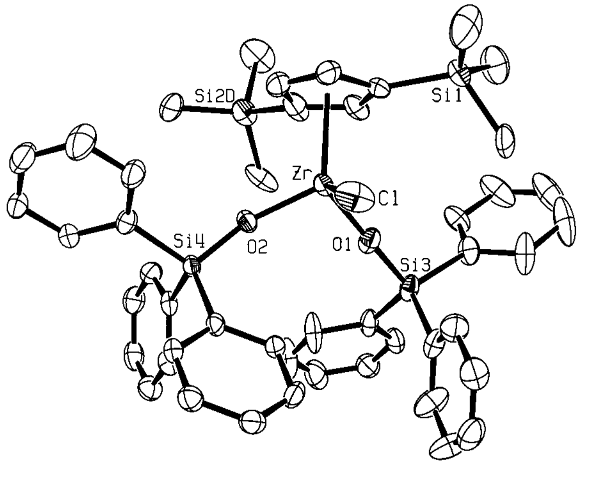

Figure 1. ORTEP drawing of Cp″[Ph$_3$SiO]$_2$ZrCl (**9**). Ellipsoids are scaled to enclose 40% of the electron density. Selected bond distances (Å): Zr−Cl, 2.392(2); Zr−O(1), 1.921(4); Zr−O(2), 1.929(5); Zr−Cg, 2.217(4). Bond angles (deg): Zr−O(1)−Si(3), 175.3(3); Zr−O(2)−Si(4), 159.3(2); Cl−Zr−O(1), 103.32(14); Cl−Zr−O(2), 102.82(13); O(1)−Zr−O(2), 102.17(19); Cl−Zr−Cg, 111.35(10); O(1)−Zr-−g, 119.05(18); O(2)−Zr−Cg, 116.15(15).

---

[15] Poor crystallinity is a general characteristic of silsesquioxane compounds: (a) Feher, F. J. *J. Am. Chem. Soc.* **1986**, *108*, 3850. (b) Feher, F. J.; Budzichowski, T. A.; Ziller, J. W. *Inorg. Chem.* **1992**, *31*, 5100. (c) Buys, I. E.; Hambley, T. W.; Houlton, D. J.; Maschmeyer, T.; Masters, A. F.; Smith, A. K. *J. Mol. Catal.* **1994**, *86*, 309.

Table 1. Details of the X-ray Structure Determination of Cp″[Ph_3SiO]$_2$ZrCl (9) and Cp″[Ph_3SiO]Ti(CH_2Ph)$_2$ (11a)

	9	11a
formula	$C_{47}H_{51}ClO_2Si_4Zr$	$C_{43}H_{50}OSi_3Ti$
fw	886.94	714.99
cryst syst	trigonal	triclinic
space group, No.	$R\bar{3}$ (H, obv.), 148	$P\bar{1}$, 2
a, Å	48.71(1)	11.461(1)
b, Å		12.709(1)
c, Å	10.998(2)	14.702(1)
α, deg		83.503(5)
β, deg		70.018(5)
γ, deg		84.972(5)
V, Å^3	22 599(8)	1996.9(3)
D_{calcd}, g cm^{-3}	1.173	1.189
Z	18	2
$F(000)$, electrons	8316	760
μ(Mo Kα), cm^{-1}	4.0	3.4
cryst size, mm	0.45 × 0.50 × 0.55	0.25 × 0.30 × 0.38
T, K	130	130
θ range, deg: min, max	1.45, 26.0	1.48, 27.0
λ(Mo Kα), Å	0.710 73	0.710 73
monochromator	graphite	graphite
$\omega/2\theta$ scan, deg	$\Delta\omega = 0.90 + 0.34 \tan\theta$	$\Delta\omega = 0.90 + 0.34 \tan\theta$
index ranges	h, 0−60; k, −59 to 0; l, 0−11	h, −13 to +14; k, −16 to 16; l, 0−18
total no. of data	10 145	9035
no. of unique data	9318	8689
no. of data with criterion $F_o \geq 4.0\sigma(F_o)$	7567	6626
$R_{\mathrm{int}} = \Sigma[\lvert(F_o^2 - F_o^2(\mathrm{mean})\rvert)/\Sigma[F_o^2]$	0.058	0.0612
$R_\sigma = \Sigma\sigma(F_o^2)/\Sigma[F_o^2]$	0.038	0.0408
no. of rflns with $F_o^2 \geq 0$	9318	8688
no. of refined params	574	633
final agreement factors		
$R_w(F^2)$ for $F_o^2 > 0$[a]	0.2354	0.1063
weighting scheme: a, b[b]	0.1099, 217.3	0.0622, 0.1390
$R(F)$ for $F_o > 4.0\sigma(F_o)$[c]	0.0785	0.0428
GOF = S[d]	1.163	1.021
max (shift/σ) final cycle	<0.001	<0.001

[a] $R_w(F^2) = [\Sigma[w(F_o^2 - F_c^2)^2]/\Sigma[w(F_o^2)^2]]^{1/2}$. [b] $w = 1/[\sigma^2(F_o^2) + (aP)^2 + bP]$ and $P = [\max(F_o^2,0) + 2F_c^2]/3$. [c] $R(F) = \Sigma(\lvert\lvert F_o\rvert - \lvert F_c\rvert\rvert)/\Sigma\lvert F_o\rvert$. [d] GOF = $S = [\Sigma[w(F_o^2 - F_c^2)^2]/(n/p)]^{1/2}$; n = number of reflections, and p = number of parameters refined.

Si_7O_{12}]ZrCp* (1.958 Å),[15a] [(c-C_5H_9)$_7$$Si_7O_{11}$($OSiMe_3$)]$_2$Zr·2THF (2.00 Å average),[7i] and {[(c-C_5H_9)$_7$$Si_7O_{12}$]Zr$CH_2$Ph}$_2$ (σ-bonded: 1.96 Å average)[7i] but compare well with the Zr−O distances in (Ph_3SiO)$_2$ZrCl_2·DME (1.91(1) Å) and electron-deficient zirconium alkoxide complexes.[16] The combination of short Zr−O distances (1.925 Å average) and nearly linear Zr−O−Si bond angles (167.3° average) in **9** provide a clear manifestation of strong oxygen pπ−dπ donation of the siloxy ligand to the zirconium center. To reduce the steric congestion within the complex, the two bulky trimethylsilyl substituents of the cyclopentadienyl ligand occupy the least crowded position between the two siloxy groups, whereas the phenyl groups of the siloxy ligands are twisted like propeller blades with an average torsion angle of 47°.

Half-Sandwich Group 4 Metal Silsesquioxane and Triphenylsiloxy Alkyl Complexes. In accordance with the grafting of group 4 metal alkyls onto partially dehydroxylated silica[5] and the alcoholysis with ROH (e.g. ROH = (Me_3C)$_3$COH, 2,6-(Me_3C)$_2$-C_6H_3OH, 2,2′-CH_2(C_6H_2-4-Me-6-(CMe_3)OH)$_2$),[16] protonolysis reactions of Ph_3SiOH and (c-C_5H_9)$_7$$Si_8O_{12}$(OH) (**2**) were carried out.[17] Reactions of Cp″TiR_3 with **2** proceed selectively, providing the corresponding mono(silsesquioxane) bis(alkyl) complexes Cp″[(c-C_5H_9)$_7$$Si_8O_{13}$]Ti$R_2$ (R = CH_2Ph (**10a**), Me (**10b**); Scheme 1). Attempts to introduce a second silsesquioxane failed, as both alkyls **10a**,**b** refuse to react with another 1 equiv of silsesquioxane **2**. Heating toluene solutions of **10a**,**b** exclusively resulted in thermolysis of the bis(alkyl) complexes. The reactivity of Ph_3SiOH toward Cp″TiR_3 corresponds surprisingly well to that of (c-C_5H_9)$_7$$Si_8O_{12}$(OH) (**2**). The triphenylsiloxy analogues of **10a**,**b**, Cp″[Ph_3SiO]TiR_2 (R = CH_2Ph (**11a**), Me (**11b**) Scheme 1), are selectively formed by treatment of CpTiR_3 (R = CH_2Ph, Me) with equimolar amounts of Ph_3SiOH. Like **10a**,**b**, the titanasiloxy complexes **11a**,**b** refuse to react with a second equivalent of Ph_3SiOH.

For zirconium, the protonolysis reaction between Cp″ZrR_3 (R = Me, CH_2Ph) and silsesquioxane **2** is much less selective than for titanium. Instead of the expected product, Cp″[(c-C_5H_9)$_7$$Si_8O_{13}$]Zr$R_2$, treatment of Cp″Zr$R_3$ with **2** invariably yields complex product mixtures. Multiple $SiMe_3$ and silsesquioxane resonances in the NMR spectra of these mixtures indicate the presence of several products of the type Cp″[(c-C_5H_9)$_7$$Si_8O_{13}$]$_x$-Zr$R_{3-x}$. The formation of these product mixtures indicates that the rate of protonolysis for the intermediate silsesquioxane metal benzyl complexes is at least of the same order as for Cp″ZrR_3. In contrast with the nonselective reactions described above, the protonolysis reaction between Cp″Zr(CH_2Ph)$_3$ and Ph_3SiOH proceeds very selectively with either 1 or 2 equiv of

---

(16) (a) Babaian, E. A.; Hrcir, D. C.; Bott, S. G.; Atwood, J. L. *Inorg. Chem.* **1986**, *25*, 4818. (b) Latesky, S. L.; McMullen, A. K.; Niccolai, G. P.; Rothwell, I. P.; Huffman, J. C. *Organometallics* **1985**, *4*, 902. (c) Lubben, T. V.; Wolczanski, P. T.; Van Duyne, G. D. *Organometallics* **1984**, *3*, 977.

(17) Alkylation (MeLi, MeMgCl, Me_2Zn, PhCH_2MgCl) of the chloride complexes **6**−**9** did not afford well-defined products.

triphenylsilanol, affording Cp″[Ph_3SiO]Zr(CH_2Ph)$_2$ (**12a**) or Cp″[Ph_3SiO]$_2$ZrCH_2Ph (**12b**, Scheme 1), respectively.

The NMR (^{1}H, ^{13}C, ^{29}Si) spectra of the titanasilsesquioxane alkyl complexes **10a**,**b** show roughly the same features as observed for the corresponding titanasilsesquioxane dichloro compound **6a**. For example, only one resonance is observed for all seven methine *C*H carbon atoms of the silsesquioxane ligand and the ^{29}Si NMR spectra of **10a**,**b** display four resonances in a 2:3:4:1 ratio. The chemical shifts of the methyl resonances of **10b** and **11b** (**10b**, ^{1}H δ 1.01 ppm, ^{13}C δ 56.56 ppm, $^1J_{C-H} = 123$ Hz; **11b**, ^{1}H δ 1.10 ppm, ^{13}C δ 55.80 ppm, $^1J_{C-H} = 128$ Hz) are virtually identical. Likewise, the chemical shifts for the methylene resonances of **10a** and **11a** are also very similar. For both dibenzyl complexes the methylene protons (TiC*HH*′) are diastereotopic, giving an AB spin system in the ^{1}H NMR spectrum (**10a**, ^{1}H δ 3.48, δ 2.16 ppm, $^2J_{H-H} = 10$ Hz; **11a**, ^{1}H δ 3.16, δ 2.22 ppm, $^2J_{H-H} = 9.9$ Hz), while the methylene (Ti*C*H_2) carbons appear as triplets (^{13}C: **10a**, δ 86.83 ppm, $^1J_{C-H} = 127$ Hz; **11a**, δ 86.1 ppm, $^1J_{C-H} = 125$ Hz). These values are comparable with those found for structurally comparable cyclopentadienyl−alkoxo complexes such as [η^5:η^1-C_5Me_4-2-C_6H_3(4-Me)O]Ti(CH_2Ph)$_2$ (^{1}H, δ 2.50, δ 2.32 ppm, $^2J_{H-H} = 10.2$ Hz; ^{13}C, δ 83.85 ppm, $^1J_{C-H} = 127.5$ Hz)[18a] and [η^5:η^1-C_5Me_4(CH_2)$_3$O]Ti(CH_2Ph)$_2$ (^{1}H, δ 2.22, δ 1.92 ppm, $^2J_{H-H} = 10.3$ Hz; ^{13}C, δ 78.35 ppm, $^1J_{C-H} = 121.2$ Hz).[18b] The normal chemical shift and $^1J_{C-H}$ value of the Ti*C*H_2 group and the absence of a high-field shift of benzyl ortho phenyl protons in **10a** and **11a** excludes significant η^2-bonding of the benzyl group.[19] In accordance with the titanium dibenzyl complexes **10a** and **11a**, the zirconium monosiloxy dibenzyl complex Cp″[Ph_3SiO]Zr(CH_2Ph)$_2$ (**12a**) shows an AB spin pattern for its diastereotopic methylene C*HH*′ protons (^{1}H: δ 2.50, δ 2.10 ppm, $^2J_{H-H} =$ 11.0 Hz) and a triplet for the methylene carbon (^{13}C: δ 63.1 ppm, $^1J_{C-H} = 124$ Hz). On the other hand, the methylene protons of the corresponding monobenzyl complex Cp″[Ph_3SiO]$_2$ZrCH_2Ph (**12b**) are identical and appear as a singlet (δ 2.84 ppm) in the ^{1}H and as a triplet (δ 59.3 ppm, $^1J_{C-H} = 119$ Hz) in the ^{13}C NMR spectrum.

X-ray Structure Determination of Cp″[Ph_3SiO]Ti(CH_2Ph)$_2$ (11a). The solid-state structure of **11a** as derived from single-crystal X-ray diffraction is shown in Figure 2. The geometry around titanium is slightly distorted tetrahedral, with an O(1)−Ti−Cp (centroid) angle of 126.64°. Clearly, this large angle results from the steric hindrance between the cyclopentadienyl and the siloxy ligand. The Ti−O(1) bond length in **11a** (1.8055(15) Å) is comparable to those reported for titanium cyclopentadienyl−alkoxide complexes, such as [η^5:η^1-C_5Me_4-2-C_6H_3(4-Me)O]Ti(CH_2Ph)$_2$ (1.851(7) Å),[18a] [η^5:η^1-C_5R_4(CH_2)$_3$O]TiCl_2 (R = H, 1.762(2) Å;[20a] R = Me, 1.767(1) Å),[20b] and C_5Me_5[2,6-(*i*-Pr)$_2C_6H_3$O]TiCl_2 (1.772(3) Å)[20c] and the titanium alkoxide complexes (2,6-$Ph_2C_6H_3O$)$_2$TiC_4H_8 (average 1.806(1) Å)[20d] and 2,2′-(4-OMe,6-*t*-BuC_6H_2O)$_2$Ti(CH_2Ph)$_2$ (average 1.810(8) Å)[20e] and siloxy complexes [(Me_3C)$_3$SiO]$_2$Ti(THF)NSiCMe_3 (1.824(4) Å), [(Me_3C)$_3$SiO]$_3$TiNH_2 (1.815 Å),[6a] and Ph_3SiOTi(OCH_2CH_2)$_3$N (1.834 Å).[21] Similar to what was observed for **9**, the partial Ti−O double-bond character and the nearly linear Ti−O(1)−Si(3) angle of 174.51(10)° reflect additional oxygen π-donation to the metal. The two benzyl ligands in **11a** are inequivalent, but can both be regarded as being η^1-bound to titanium, which is in agreement with the solution ^{1}H and ^{13}C NMR spectra of **11a**.

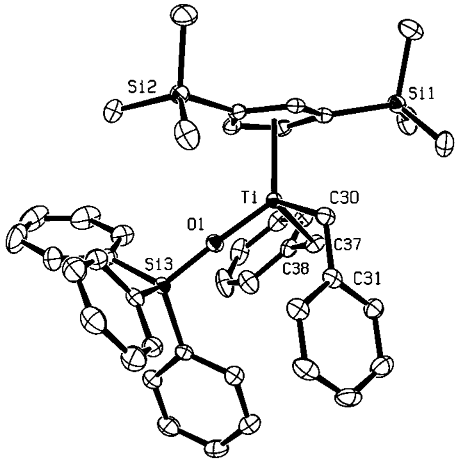

Figure 2. ORTEP drawing of Cp″[Ph_3SiO]Ti(CH_2Ph)$_2$ (**11a**). Ellipsoids are scaled to enclose 40% of the electron density. Selected bond distances (Å): Ti−O(1), 1.8055(15); Ti−C(30), 2.140(2); Ti−C(37), 2.145(2); Ti−Cg, 2.0644(11). Bond angles (deg): Ti−O(1)−Si(3), 174.51(10); Ti−C(30)−C(31), 113.54(14); Ti−C(37)−C(38), 118.49(15); O(1)−Ti−C(30), 102.37(8); O(1)−Ti-C(37), 101.58(8); C(30)−Ti−C(37), 102.23(8); O(1)−Ti−Cg, 126.64(5); C(30)−Ti−Cg, 109.14(8); C(37)−Ti−Cg, 112.02(8).

Olefin Polymerization and Catalyst Stability. Olefin polymerization experiments of the described metallasilsesquioxane and metallasiloxane chloro and alkyl complexes have been carried out. Besides polymerization activity studies, possible "leaching" of the complexes was also investigated.

With MAO as the cocatalyst, not only do the dichloride complexes Cp″[(*c*-C_5H_9)$_7Si_8O_{13}$]MCl_2 (M = Ti (**6a**), Zr (**7a**)) and Cp″[Ph_3SiO]TiCl_2 (**8a**) generate active ethylene polymerization catalysts but also the corresponding monochlorides Cp″[(*c*-C_5H_9)$_7Si_8O_{13}$]$_2$MCl (M = Ti (**6b**), Zr (**7b**)) and Cp″[Ph_3SiO]$_2$MCl (M = Ti (**8b**), Zr (**9**)) polymerize ethylene.[22] Obviously, the monochloride

---

[18] (a) Chen, Y.-X.; Fu, P.-F.; Stern, C.; Marks, T. J. *Organometallics* **1997**, *16*, 5958. (b) Gielens, E. E. C. G.; Tiesnitsch, J. Y.; Hessen, B.; Teuben, J. H. *Organometallics* **1998**, *17*, 1652.

[19] For example, see: (a) Bochmann, M.; Lancaster, S. J.; Hursthouse, M. B.; Malik, K. M. A. *Organometallics* **1994**, *13*, 2235 and references therein. (b) Horton, A. D.; de With, J.; van der Linden, A. J.; van de Weg, H. *Organometallics* **1996**, *15*, 2672. (c) Pellecchia, C.; Immirzi, A.; Grassi, A.; Zambelli, A. *Organometallics* **1993**, *12*, 4473.

[20] (a) Trouvé, G.; Laske, D. A.; Meetsma, A.; Teuben, J. H. *J. Organomet. Chem.* **1996**, *511*, 255. (b) Fandos, R.; Meetsma, A.; Teuben, J. H. *Organometallics* **1991**, *10*, 59. (c) Nomura, K.; Naga, N.; Miki, M.; Yanagi, K.; Imai, A. *Organometallics* **1998**, *17*, 2154. (d) Thorn, M. G.; Hill, J. E.; Waratuke, S. A.; Johnson, E. S.; Fanwick, P. E.; Rothwell, I. P. *J. Am. Chem. Soc.* **1997**, *119*, 8630. (e) van der Linden, A.; Schaverien, C. J.; Meijboom, N.; Ganter, C.; Orpen, A. G. *J. Am. Chem. Soc.* **1995**, *117*, 3008.

[21] Menge, W. M. P. B.; Verkade, J. G. *Inorg. Chem.* **1991**, *30*, 4628.

[22] Conditions: 20 mmol of MAO; 20 μmol of catalyst; 5 atm of ethylene, 80 °C, 7 min. Observed activities range between 0.4 and 1.2 kg of PE/ (mmol[cat] h atm), based on the polymer yield after 7 min.

complexes can only yield active ethylene polymerization catalysts when at least one of the silsesquioxane or siloxy ligands is substituted. This clearly demonstrates the poor stability of monodentate siloxy systems toward substitution by aluminum alkyls.[23] To test whether the chelate effect of silsesquioxane ligands might improve the stability toward leaching, titanium and zirconium precursors with tridentate silsesquioxane ligands have been synthesized, $[(c\text{-}C_5H_9)_7Si_7O_{12}]MCp''$ (M = Ti (**13**), Zr (**14**); eq 2).[24]

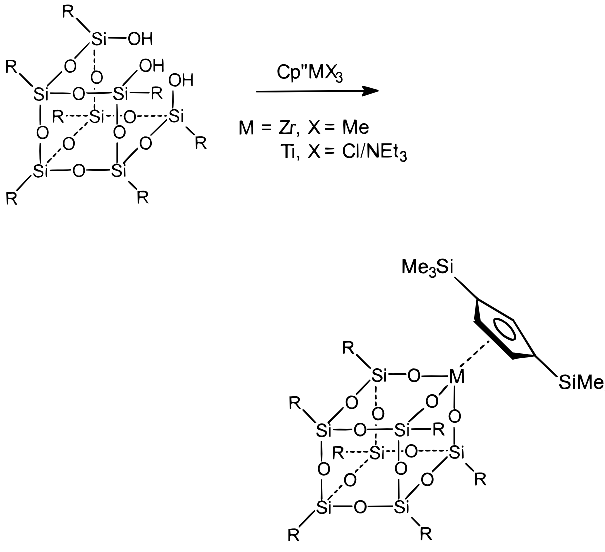

M = Ti (**13**), Zr (**14**)

(2)

The fact that even solutions of **13** and **14** treated with MAO give active ethylene polymerization catalysts[22] excludes any positive influence of the chelate effect of the silsesquioxane ligands on the stability toward leaching. Worth mentioning in this respect is a study by Feher et al., who demonstrated that with equimolar amounts of aluminum alkyls two of the three V−O bonds in the vanadasilsesquioxane $[(c\text{-}C_6H_{11})_7Si_7O_{12}]V{=}O$ are selectively split.[7b,d] Hence, the high affinity of aluminum for silsesquioxane oxo functionalities makes aluminum alkyls unsuitable as cocatalysts for these systems, when used in excess. The facile activation of **6b**/**7b** and **13**/**14** also gives rise to considerable doubt about the stability of the M−O bonds in silica-grafted mono(cyclopentadienyl) systems,[1g,10] in the presence of excess of aluminum alkyls. This is emphasized by Soga et al.,[10d] who showed that significant amounts of titanium dissolve in the solution in which the silica-supported $(C_5Me_5)TiCl_3$ is treated with MAO.

When activated with $B(C_6F_5)_3$, the titanium bis(alkyl) complexes **10** and **11** form active olefin polymerization catalysts (Table 2). Ethylene was polymerized rapidly, and 1-hexene was slowly transformed into atactic poly-1-hexene (Table 2). The narrow molecular weight distributions of the poly-1-hexenes formed indicate that both **10a** and **11a** form single-site catalysts when activated with $B(C_6F_5)_3$.[25] The somewhat broader molecular weight distributions of the polyethylenes formed can be explained by partial thermolysis of the catalysts under the conditions applied (80 °C). The zirconium dibenzyl complex **12a** forms a very poor catalyst when activated with $B(C_6F_5)_3$. Ethylene was polymerized only slowly, while 1-hexene was not polymerized at all. To test whether $B(C_6F_5)_3$ is capable of substituting silsesquioxane or triphenylsiloxy ligands, ^{19}F NMR studies were carried out on solutions of $Cp''[(c\text{-}C_5H_9)_7Si_8O_{13}]_2TiCl$ (**6b**) and $Cp''[Ph_3SiO]_2TiCl$ (**8b**) with $B(C_6F_5)_3$. As expected, the ^{19}F NMR spectra exclusively showed unreacted $B(C_6F_5)_3$.

Table 2. Polymerization Results of $B(C_6F_5)_3$ Activated Systems

catalyst (amt, μmol)	monomer	yield (g)	activity (kg/(mol h atm))	M_w ($\times10^{-3}$)	M_w/M_n
10a (20)[a]	ethylene	10.2	880	260	3.3
10b (20)[a]	ethylene	9.8	840		
11a (20)[a]	ethylene	26.2	2240	440	2.9
11b (20)[a]	ethylene	17.0	1460	360	3.7
12a (40)[b]	ethylene	0.6	3		
10a (20)[c]	1-hexene	4.5	3	2.9	2.0
11a (20)[c]	1-hexene	5.8	4	11.0	2.1

[a] Conditions: 1 mmol of $B(C_6F_5)_3$, 80 °C, 7 min, 5 atm of ethylene. [b] Conditions: 1 mmol $B(C_6F_5)_3$, 80 °C, 1 h, 5 atm of ethylene. [c] Conditions: 0.2 mmol of $B(C_6F_5)_3$, 25 °C, 16 h, neat 1-hexene.

Steric and Electronic Properties of $(c\text{-}C_5H_9)_7Si_8O_{12}(OH)$ and Ph_3SiOH. Although simple silanols have been assumed to be less suitable models for silica than silsesquioxanes,[7f,26] the reactivity of Ph_3SiOX and $(c\text{-}C_5H_9)_7Si_8O_{13}X$ (X = H, Li/Tl) toward $Cp''MX_3$ (M = Ti, Zr; X = Cl, alkyl) shows some remarkable similarities, though some distinct differences could be observed as well. To get insight into the steric and electronic differences between Ph_3SiOH and $(c\text{-}C_5H_9)_7Si_8O_{12}(OH)$, and to assess their suitability as models for silica surface silanol sites, the steric and electronic properties of both ligands were investigated in more detail using molecular modeling, DFT calculations, and pK_a measurements.

To determine the steric bulk of both $(c\text{-}C_5H_9)_7Si_8O_{12}(OH)$ (**2**) and Ph_3SiOH, CPK models (Figure 3) have been built using molecular modeling (force field). Both ligands are C_3 symmetric, which makes the comparison of cone angles more reliable. On the basis of the cone angles of $(c\text{-}C_5H_9)_7Si_8O_{13}$ (155°) and Ph_3SiO (132°),[27] it is clear that silsesquioxane **2** is considerably larger than triphenylsilanol. However, describing the steric bulk of a system on the basis of cone angles alone is often not sufficient. For example, in complexes containing silsesquioxane **2** the cyclopentyl substituents are located

---

(23) This is not very surprising, since $CpTi(OBu)_3$/MAO and $Cp^*Ti(OCH_2CH_2)_3N$/MAO are known styrene polymerization catalysts, indicating that Ti−O bonds can be split by MAO: (a) Chien, J. C. W.; Salajka, Z. *J. Polym. Sci., Part A: Polym. Chem.* **1991**, *29*, 1253. (b) Kim, Y.; Hong, E.; Lee, M. H.; Kim, J.; Han, Y.; Do, Y. *Organometallics* **1999**, *18*, 36.

(24) (a) Feher, F. J. *J. Am. Chem. Soc.* **1986**, *108*, 3850. (b) Buys, I. E.; Hambley, T. W.; Houlton, D. J.; Maschmeyer, T.; Masters, A. F.; Smith, A. K. *J. Mol. Catal.* **1994**, *86*, 309.

(25) ^{19}F NMR spectroscopy (toluene-d_8, 25 °C) showed that treatment of **10a** with $B(C_6F_5)_3$ affords a contact ion pair with $[PhCH_2B(C_6F_5)_3]^-$ (^{19}F NMR (δ): −53.0, (F_o), −83.80 (F_p), −87.80 (F_m) ppm; $\Delta\delta(F_m-F_p)$ = 4.0 ppm), whereas the reaction of **11a** with $B(C_6F_5)_3$ yields a solvent-separated ion pair (^{19}F NMR (δ): −53.0 (F_o), −87.1 (F_p), −89.7 (F_m) ppm; $\Delta\delta(F_m-F_p)$ = 2.6 ppm). See also ref 19b. The ^1H NMR spectra (toluene-d_8) were not very informative, as broad signals were observed at both −45 and +25 °C.

(26) Feher, F. J.; Newman, D. A.; Walzer, J. F. *J. Am. Chem. Soc.* **1989**, *111*, 1741.

(27) As input for the calculations, force field optimized structures of the ligands were used, to which a Ti atom was attached at 1.85 Å, with a Si−O−Ti angle of 180°. The cone angles were calculated using a modified version of Steric: Taverner, B. C. *J. Comput. Chem.* **1996**, *14*, 1612.

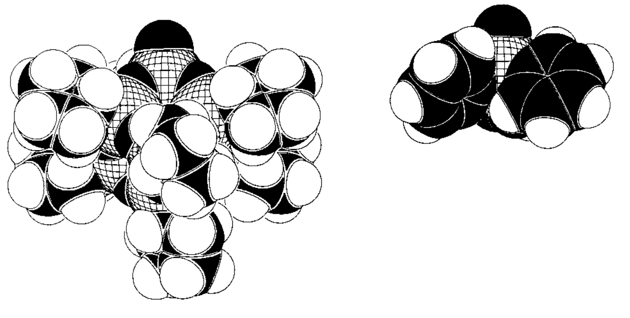

Figure 3. CPK models for (c-$C_5H_9)_7Si_8O_{13}$ and Ph_3SiO siloxy fragments.

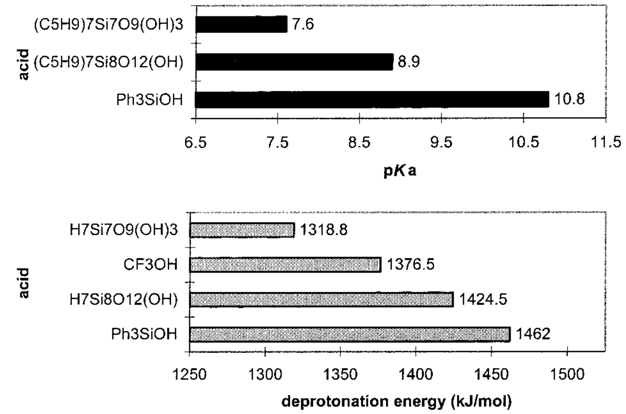

Figure 4. pK_a values and calculated deprotonation energies.

approximately 1 Å further away from the metal center than the phenyl groups in the corresponding triphenylsiloxy compounds (Figure 3). As a result, the effective steric congestion around the metal centers in both systems is less different than assumed on the basis of cone angles alone. This assumption is supported by the similar selectivities of the chloride metathesis reactions of $[(c\text{-}C_5H_9)_7Si_8O_{13}]Li$ and Ph_3SiOTl with $Cp''MCl_3$ (M = Ti, Zr; vide supra) and the lack of both **10a** and **11a** to react with another 1 equiv of $(c\text{-}C_5H_9)_7Si_8O_{12}(OH)$ and Ph_3SiOH, respectively.

Feher et al. have reported that, unlike usual silanols, silsesquioxanes are strongly electron-withdrawing ligands with an electrophilicity resembling that of corresponding silica surface silanol sites. The electron-withdrawing capacity of the silsesquioxane in the Schrock-type alkylidene complex $[(c\text{-}C_6H_{11})_7Si_7O_{11}(OSiMe_3)]Mo(CHCMe_2Ph)(NAr)$ resembles that of the two $(CF_3)_2(CH_3)CO$ ligands in $[(CF_3)_2(CH_3)CO]Mo(CHCMe_2Ph)(NAr)$.[7d] However, on the basis of Hammett correlations, the electron-withdrawing tendency of the $[Si_8O_{12}]$ framework in aryl-substituted silsesquioxanes was even found to approach that of a trifluoromethyl group.[28] To study the electronic character of Ph_3SiOH and $(c\text{-}C_5H_9)_7Si_8O_{12}(OH)$, more direct methods to determine the electronic properties of these ligands were sought.

As there is a clear correlation between the electron-withdrawing tendency of the R substituent and the acidity of ROH, the Brønsted acidities of Ph_3SiOH and $(c\text{-}C_5H_9)_7Si_8O_{12}(OH)$ (**2**) were determined by pK_a measurements.[29] Subsequently, these pK_a values were compared with the calculated deprotonation energies of the silanols. The pK_a measurements were performed in THF using the overlapping indicator method,[29b−f] and the deprotonation energies are the result of DFT calculations for the silanols at 0 K under vacuum.[30]

As can be seen from Figure 4, Ph_3SiOH is significantly less Brønsted acidic than $(c\text{-}C_5H_9)_7Si_8O_{12}(OH)$ (**2**). Interesting to note is the difference in acidity between $(c\text{-}C_5H_9)_7Si_8O_{12}(OH)$ (**2**) and the tris(silanol) $(c\text{-}C_5H_9)_7Si_7O_9(OH)_3$ (vide infra), which resembles the difference in acidity of isolated silanols and silanol nests in zeolitic materials.[31] The pK_a values are in good agreement with the calculated deprotonation energies for $H_7Si_7O_9(OH)_3$, $H_7Si_8O_{12}(OH)$, and Ph_3SiOH, respectively.[32] The deprotonation energy for $H_7Si_8O_{12}(OH)$ is significantly higher than for CF_3OH ($\Delta E = 47.9$ kJ mol^{-1}). Hence, on the basis of these calculations, the electron-withdrawing capacity of the $[Si_8O_{12}]$ framework is less pronounced than is found on the basis of Hammett correlations[28] and is intermediate between those of the Ph_3Si and the CF_3 substituent. Surprisingly, the calculated deprotonation energy of the tris(silanol) $H_7Si_7O_9(OH)_3$ was found to be even lower than that of CF_3OH. DFT calculations show that the high acidity of $(c\text{-}C_5H_9)_7Si_7O_9(OH)_3$ is the result of effective stabilization of the charge in the conjugated base $[(c\text{-}C_5H_9)_7Si_7O_{10}(OH)_2]^-$ by means of intramolecular hydrogen bridges.[30] The strong acidity of $(c\text{-}C_5H_9)_7Si_7O_9(OH)_3$ and corresponding high stability of the monoanion $[(c\text{-}C_5H_9)_7Si_7O_{10}(OH)_2]^-$ explain the fact that silylation of the first hydroxyl group in $(c\text{-}C_5H_9)_7Si_7O_9(OH)_3$ was found to be approximately 3 orders of magnitude faster than subsequent silylation of the second and third silanols.[33]

As a second approach to estimate the electron-withdrawing tendency of silanol ligands, the protonation energy of $L(L')TiH_2$ was calculated. Strong electron-withdrawing ligands L and L′ will hamper hydride abstraction from $L(L')TiH_2$, as these ligands are less able to stabilize the corresponding cation $L(L')TiH^+$. We used this model reaction to investigate how alkyl abstraction of a titanium bis(alkyl) complex by e.g. $B(C_6F_5)_3$ is influenced by the electron-withdrawing capacity of the ancillary ligands.[34]

As can be seen from Figure 5, the energy required to remove a hydride from complexes containing CF_3O ancillary ligands is substantially higher than for the

---

(28) Feher, F. J.; Budzichowski, T. A. *J. Organomet. Chem.* **1989**, *379*, 33.

(29) (a) Cookson, R. F. *Chem. Rev.* **1974**, *74*, 5. (b) Matthews, W. S.; Bares, J. E.; Bartmess, J. E.; Bordwell, F. G.; Cornforth, F. J.; Drucker, G. E.; Margolin, Z.; McCallum, R. J.; McCollum, G. J.; Vanier, N. R. *J. Am. Chem. Soc.* **1975**, *97*, 7006. (c) Olmstread, W. N.; Bordwell, F. G. *J. Org. Chem.* **1980**, *45*, 3299. (d) Bordwell, F. G.; McCallum, R. J.; Olmstead, W. N. *J. Org. Chem.* **1984**, *49*, 1424. (e) Kaufmann, M. J.; Streitwieser, A., Jr. *J. Am. Chem. Soc.* **1987**, *109*, 6092. (f) Bordwell, F. G. *Acc. Chem. Res.* **1988**, *21*, 456 and references therein.

(30) A detailed discussion about pK_a values and calculated deprotonation energies of silsesquioxanes will be reported elsewhere: Harmsen, R. J.; Duchateau, R.; Krijnen, S.; van Santen, R. A. Manuscript in preparation.

(31) For example, see: Kramer, G. J.; van Santen, R. A.; Emeis, C. A.; Nowak, A. K. *Nature* **1993**, *363*, 529 and references therein.

(32) To reduce DFT calculation time, the silsesquioxane cyclopentyl substituents were replaced by hydrogens.

(33) (a) Feher, F. J.; Newman, D. A. *J. Am. Chem. Soc.* **1990**, *112*, 1931. (b) Feher, F. J.; Phillips, S. H.; Ziller, J. W. *Chem. Commun.* **1997**, 829.

(34) The cationic titanium species $[(C_5Me_5)Ti(OC_6F_5)_2]^+$ was found to effectively compete with $B(C_6F_5)_3$ for the alkyl group: Tremblay, T. L.; Ewart, S. W.; Sarsfield, M. J.; Baird, M. C. *Chem. Commun.* **1997**, 831.

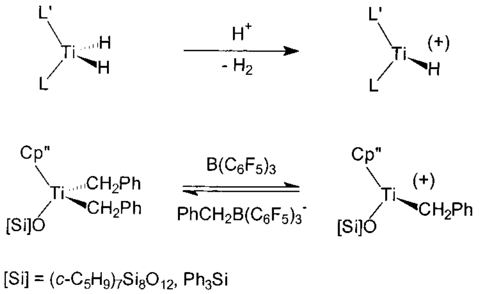

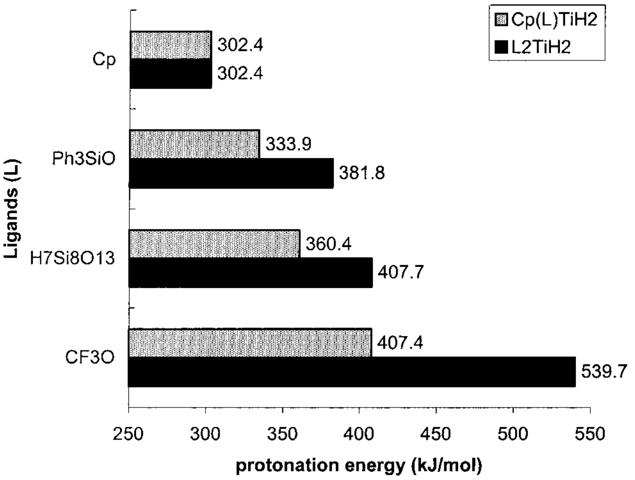

Figure 5. Protonation energies of L_2TiH_2 and $Cp(L)TiH_2$ for different ligands L.

corresponding compounds stabilized by $H_7Si_8O_{13}$ or Ph_3SiO ligands, which indicates that CF_3O is more electron-withdrawing than both siloxides, $H_7Si_8O_{13}$ and Ph_3SiO. Protonolysis of $[H_7Si_8O_{13}]_2TiH_2$ and $Cp[H_7Si_8O_{13}]TiH_2$ is also more difficult than for $[Ph_3SiO]_2TiH_2$ and $Cp[Ph_3SiO]TiH_2$, respectively, indicating that the silsesquioxane $H_7Si_8O_{13}$ ligand is less electron donating than the Ph_3SiO ligand. However, the energy differences are notably smaller in comparison with the CF_3O-containing systems. The outcome of these calculations corresponds well with the lower deprotonation energy and pK_a value of $H_7Si_8O_{12}(OH)$ compared to Ph_3SiOH.

In an attempt to confirm these calculated energy differences, dibenzyl complexes $Cp[(c\text{-}C_5H_9)_7Si_8O_{13}]Ti(CH_2Ph)_2$ (**10a**) and $Cp''[Ph_3SiO]Ti(CH_2Ph)_2$ (**11a**) were treated with $B(C_6F_5)_3$. The ^{19}F NMR spectra showed distinct resonances of both $B(C_6F_5)_3$ and $[PhCH_2B(C_6F_5)_3]^-$.[25] For an equimolar mixture of **10a** + $B(C_6F_5)_3$, the $B(C_6F_5)_3$:$[PhCH_2B(C_6F_5)_3]^-$ ratio was found to be 1:1. With a $B(C_6F_5)_3$:$[PhCH_2B(C_6F_5)_3]^-$ ratio of 0.2:1 for an equimolar mixture of **11a** + $B(C_6F_5)_3$, benzyl abstraction is more facile for the triphenylsilyl system than for the corresponding silsesquioxane system. Clearly, both Lewis acids $[Cp[(c\text{-}C_5H_9)_7Si_8O_{13}]TiCH_2Ph]^+$ and $[Cp''[Ph_3SiO]TiCH_2Ph]^+$ effectively compete with $B(C_6F_5)_3$ for possession of the benzyl group.[34] Although steric factors cannot be excluded, these results are in agreement with the calculated energy difference for the hydride abstraction of $Cp[H_7Si_8O_{13}]TiH_2$ and $Cp[Ph_3SiO]TiH_2$ and indicate that the triphenylsilyl ligand is less electron withdrawing than the silsesquioxane.

Concluding Remarks

A new class of group 4 metal compounds has been developed, which provides catalyst precursors for the polymerization of olefins and serves as a well-defined model for corresponding silica-grafted surface complexes. Due to their high affinity for the siloxy/silsesquioxane oxo functionalities, aluminum alkyls are, when used in excess, unsuitable cocatalysts/scavengers for siloxy and silsesquioxane complexes and probably also for the corresponding silica-grafted systems. On the other hand, triphenylsiloxy- and silsesquioxane-stabilized bis(alkyl) complexes (**10a**,**b**, **11a**,**b**, **12a**) proved to be active olefin polymerization catalysts when activated with $B(C_6F_5)_3$. This gives rise to promising perspectives for their silica-supported analogues when activated with boron-based cocatalysts.

The reactivities of silsesquioxane- and triphenylsilyl-stabilized group 4 metal complexes proved to be quite similar. Although the different cone angles of $(c\text{-}C_5H_9)_7Si_8O_{13}$ and Ph_3SiO suggest otherwise, the effective steric congestion around the metal center of $(c\text{-}C_5H_9)_7Si_8O_{13}$- and Ph_3SiO-stabilized complexes was found to be reasonably comparable. Silsesquioxane $(c\text{-}C_5H_9)_7Si_8O_{12}(OH)$ (**2**) is notably more Brønsted acidic than Ph_3SiOH. DFT calculations also show that silsesquioxane **2** is more electron withdrawing than Ph_3SiO. However, **2** is substantially less electron-withdrawing than a CF_3 substituent, as was found for the $[Si_8O_{12}]$ framework in $(XC_6H_4)_8Si_8O_{12}$.[28] Although silsesquioxane **2** is probably a slightly better homogeneous model for electrophilic, isolated silica surface silanols compared to the less Brønsted basic, more electron rich Ph_3SiOH, the differences in electronic properties between **2** and Ph_3SiOH are quite small. Much larger differences are observed when comparing Ph_3SiOH with the tris(silanol) $(c\text{-}C_5H_9)_7Si_7O_9(OH)_3$, which is significantly more Brønsted acidic than both Ph_3SiOH and $(c\text{-}C_5H_9)_7Si_8O_{12}(OH)$. This is in line with the higher acidity of silanol nests compared to isolated silanols in silicates and zeolites.

Experimental Section

General Considerations. All manipulations were performed under an argon atmosphere using glovebox (Braun MB-150 GI) and Schlenk techniques. Solvents were distilled from Na (toluene), K (THF), Na/K alloy (ether, hexanes), or CaH_2 (CH_2Cl_2) and stored under argon. NMR solvents were dried over Na/K alloy (benzene-d_6) or 4 Å molecular sieves ($CDCl_3$). NMR spectra were recorded on Varian Gemini 300 (^1H, 300 MHz; ^{13}C, 75.4 MHz) and Bruker AC400 (^{29}Si, 79.5 MHz) spectrometers. Chemical shifts are reported in ppm and referenced to residual solvent resonances (^1H, ^{13}C NMR) or external TMS (^{29}Si NMR) or CF_3CO_2H (^{19}F NMR). The IR spectrum of **2** was recorded on a Hitachi 270-30 spectrophotometer. Elemental analyses were carried out at the Analytical Departments of the University of Groningen (The Netherlands). To reduce the often-observed silicon carbide formation, V_2O_5 was added to improve the combustion. Titanium and zirconium analyses were performed using complexometry. The mass spectrum (FAB, matrix *m*-nitrobenzyl alcohol) of **2** was measured on a Finnigan MAT-90 high-resolution doublefocusing mass spectrometer at the Analytical Department of the University of Twente (Twente, The Netherlands). The molecular weights and molecular weight distributions were measured at 135 °C by gel permeation chromatography (GPC) (GPC210, Polymer Labs) at the University of Groningen, using 1,2,4-trichlorobenzene as solvent. $(c\text{-}C_5H_9)_7Si_7O_9(OH)_3$,[26] (*c*-

$C_5H_9)_7Si_7O_9(OSiMe_3)(OH)_2$,[35] Ph_3SiOTl,[13b] and $Cp''MX_3$ (M = Ti, Zr; X = Cl, CH_2Ph, Me)[36] were prepared by following literature procedures. Ph_3SiOH (Aldrich) was used as purchased.

$(c\text{-}C_5H_9)_7Si_8O_{12}Cl$ (1). To a suspension of $(c\text{-}C_5H_9)_7Si_7(OH)_3$ (6.96 g, 7.95 mmol) in ether (300 mL) and NEt_3 (3.3 mL, 23.8 mmol) was added $SiCl_4$ (0.9 mL, 7.86 mmol) at room temperature. The mixture was refluxed overnight and then filtered to remove $Et_3N(H)Cl$. The salt was washed with ether (2 × 30 mL), and evaporation of the filtrate yielded crude **1** as a white powder (6.85 g, 7.31 mmol, 92%). Cooling of a hot saturated toluene/acetonitrile solution afforded **1** as microcrystals. ^1H NMR ($CDCl_3$, δ): 1.72 (m, 14H, CH_2-C_5H_9), 1.55 (m, 42H, CH_2-C_5H_9), 1.05 (m, 7H, CH-C_5H_9). $^{13}C\{^1H\}$ NMR ($CDCl_3$, δ): 27.23, 27.18, 26.99, 26.90 (CH_2-C_5H_9), 22.12, 22.05, 21.85 (CH-C_5H_9, 1:3:3). ^{29}Si NMR (CH_2Cl_2, δ): −66.28, −66.85, −66.98, −90.20 (3:3:1:1). Anal. Calcd for $C_{35}H_{63}ClO_{12}Si_8$: C, 44.91; H, 6.78. Found: C, 44.85; H, 6.95.

$(c\text{-}C_5H_9)_7Si_8O_{12}(OH)$ (2). A suspension of $(c\text{-}C_5H_9)_7Si_8O_{12}Cl$ (**1**; 2.11 g, 2.25 mmol) in THF/H_2O (2:1, 50 mL) was refluxed for 40 h. Evaporation of the volatiles afforded crude **2** as a white solid. To remove the lattice THF, the product was dissolved in toluene (5 mL) and subsequently dried under vacuum. Thorough drying and recrystallization from a hot toluene/acetonitrile mixture gave **2** as a white microcrystalline material (1.65 g, 1.80 mmol, 80%). IR (Nujol, cm^{-1}): 3650 (br, OH). ^1H NMR ($CDCl_3$, δ): 2.93 (s broad, 1H, OH), 1.79 (m, 14H, CH_2-C_5H_9), 1.55 (m, 42H, CH_2-C_5H_9), 1.05 (m, 7H, CH-C_5H_9). $^{13}C\{^1H\}$ NMR ($CDCl_3$, δ): 27.25, 26.98, 26.92 (CH_2-C_5H_9), 22.17, 22.12, 22.05 (CH-C_5H_9, 1:3:3). ^{29}Si NMR (CH_2Cl_2, δ): −63,48, −64.18, −97.75 (4:3:1). A satisfactory combustion analysis simply could not be obtained. One possible explanation is the formation of refractory silicon carbides. Anal. Calcd for $C_{35}H_{64}O_{13}Si_8$: C, 45.81; H, 7.03. Found: C, 44.87; H, 7.09. Mass (FAB-nitrobenzyl alcohol): 917 (M^+), 847 (M − H − C_5H_9), 777 (M − H − 2 × C_5H_9), 709 (M − H − 3 × C_5H_9).

$[(c\text{-}C_5H_9)_7Si_8O_{13}]Tl$ (3). To a solution of **2** (3.5 g, 3.8 mmol) in toluene (25 mL) was added TlOEt (0.27 mL, 3.8 mmol) at room temperature. The mixture was left overnight, after which the volatiles were removed under vacuum, leaving crude **3** as a white foam. Recrystallization at −30 °C from hexane yielded **3** as thin colorless needles (2.2 g, 1.96 mmol, 52%). ^1H NMR ($CDCl_3$, δ): 1.78 (m, 14H, CH_2-C_5H_9), 1.54 (m, 42H, CH_2-C_5H_9), 1.00 (m, 7H, CH-C_5H_9). $^{13}C\{^1H\}$ NMR ($CDCl_3$, δ): 27.36, 27.32, 27.21, 27.07 (CH_2-C_5H_9), 22.33, 22.30, 22.27 (CH-C_5H_9, 3:1:3). ^{29}Si NMR (CH_2Cl_2, δ): −67.06, −67.31, −101.23 (4:3:1). Anal. Calcd for $C_{35}H_{63}O_{13}Si_8Tl$: C, 37.50; H, 5.67. Found: C, 37.64; H, 5.65.

$\{[(c\text{-}C_5H_9)_7Si_8O_{13}]Li\}_n$ (4). At room temperature, *n*-BuLi (0.9 mL, 2.5 M in hexanes, 2.25 mmol) was added to a solution of **2** (2.08 g, 2.27 mmol) in hexanes (50 mL). After the mixture was stirred for 0.5 h, the solvent was evaporated, leaving **4** as a white foam (1.87 g, 2.0 mmol, 89%). Due to the extreme solubility of **4** in common organic solvents, purification by means of recrystallization proved to be impossible. ^1H NMR ($CDCl_3$, δ): 1.78 (m, 14H, CH_2-C_5H_9), 1.50 (m, 42H, CH_2-C_5H_9), 0.94 (m, 7H, CH-C_5H_9). $^{13}C\{^1H\}$ NMR ($CDCl_3$, δ): 27.37, 27.29, 27.01 (CH_2-C_5H_9), 22.26, 22.21, 22.09 (CH-C_5H_9).

$[(c\text{-}C_5H_9)_7Si_8O_{13}]Li\cdot TMEDA$ (5). A room-temperature solution of **2** (4.38 g, 4.77 mmol) in ether (30 mL) was treated with BuLi (1.9 mL, 4.75 mmol, 2.5 M in hexanes). A few minutes after TMEDA (1.5 mL, 10 mmol) was added, needle-shaped crystals of **5** started to form. Subsequent cooling to 4 °C yielded **5** as colorless crystals (1.72 g, 1.65 mmol, 35%). ^1H NMR ($CDCl_3$, δ): 2.38 (s, 4H, CH_2-TMEDA), 2.32 (s, 12H, CH_3-TMEDA), 1.75 (m, 14H, CH_2-C_5H_9), 1.52 (m, 42H, CH_2-C_5H_9), 0.96 (m, 7H, CH-C_5H_9). ^{13}C NMR ($CDCl_3$, δ): 56.86 (t, CH_2-TMEDA, $^1J_{C-H} = 133$ Hz), 45.86 (q, CH_3-TMEDA, $^1J_{C-H} = 137$ Hz). $^{13}C\{^1H\}$ NMR ($CDCl_3$, δ): 27.74, 27.34, 27.28, 27,18, 27.07 (CH_2-C_5H_9), 22.71, 22.41 (CH-C_5H_9). ^{29}Si NMR (toluene, δ): −66.75, −68.35, −103.67 (4:3:1). Anal. Calcd for $C_{41}H_{79}LiN_2O_{13}Si_8$: C, 47.36; H, 7.66. Found: C, 47.00; H, 7.74.

$Cp''[(c\text{-}C_5H_9)_7Si_8O_{13}]TiCl_2$ (6a). BuLi (3.4 mL, 2.5 M in hexanes, 8.5 mmol) was added to a hexane solution of **2** (7.7 g, 8.4 mmol). Subsequently, $Cp''TiCl_3$ (3.07 g, 8.44 mmol) was added to the in situ prepared solution of $[(c\text{-}C_5H_9)_7Si_8O_{13}]Li$ and the mixture was stirred overnight at room temperature. Filtration, concentration, and cooling to −30 °C yielded a yellow powder consistent with a 9:1 mixture of **6a** and **6b**, as determined by ^1H NMR analysis. Repeated recrystallization from hexane yielded analytically pure **6a** (5.3 g, 4.3 mmol, 51%). ^1H NMR ($CDCl_3$, δ): 7.10 (s, 1H, $C_5H_3(SiMe_3)_2$), 7.02 (s, 2H, $C_5H_3(SiMe_3)_2$), 1.63 (m, 14H, CH_2-C_5H_9), 1.37 (m, 42H, CH_2-C_5H_9), 0.87 (m, 7H, CH-C_5H_9), 0.21 (s, 18H, $Si(CH_3)_3$). $^{13}C\{^1H\}$ NMR ($CDCl_3$, δ): 141.42 ($C_5H_3(SiMe_3)_2$), 132.97 ($C_5H_3(SiMe_3)_2$), 129.81 ($C_5H_3(SiMe_3)_2$), 27.31, 27.24, 27.00 (CH_2-C_5H_9), 22.12 (CH-C_5H_9), −0.59 ($Si(CH_3)_3$). ^{29}Si NMR (THF, δ): −5.63 ($SiMe_3$), −65.92, −66.66, −111.76 (2:3:4:1). Anal. Calcd for $C_{46}H_{84}Cl_2O_{13}Si_{10}Ti$: C, 44.38; H, 6.80; Ti, 3.85. Found: C, 44.20; H, 6.87; Ti, 3.85.

$Cp''[(c\text{-}C_5H_9)_7Si_8O_{13}]_2TiCl$ (6b). A solution of **4** (4.2 g, 4.6 mmol) in hexane (50 mL) was treated with $Cp''TiCl_3$ (0.79 g, 2.17 mmol), and the resulting suspension was stirred for 2 days at room temperature. The salt was removed by centrifuge, and the solvent was evaporated, yielding **6b** (3.6 g, 1.7 mmol, 78%) as a bright yellow foam. ^1H NMR ($CDCl_3$, δ): 7.23 (s, 1H, $C_5H_3(SiMe_3)_2$), 7.04 (s, 2H, $C_5H_3(SiMe_3)_2$), 1.83 (m, 28H, CH_2-C_5H_9), 1.55 (m, 84H, CH_2-C_5H_9), 1.04 (m, 14H, CH-C_5H_9), 0.38 (s, 18H, $Si(CH_3)_3$). $^{13}C\{^1H\}$ NMR ($CDCl_3$, δ): 136.44 ($C_5H_3(SiMe_3)_2$), 131.51 ($C_5H_3(SiMe_3)_2$), 127.85($C_5H_3(SiMe_3)_2$), 27.31, 27.27, 27.09, 27.04 (CH_2-C_5H_9), 22.26, 22.21, 22.11 (1:3:3, CH-C_5H_9), −0.49 ($Si(CH_3)_3$). ^{29}Si NMR (toluene, δ): −6.54 ($SiMe_3$), −65.99, −66.54, −111.25 (1:3:4:1). Anal. Calcd for $C_{81}H_{147}ClO_{26}Si_{18}Ti$: C, 45.76; H, 6.97; Ti, 2.25. Found: C, 45.36; H, 7.07; Ti, 2.19.

$Cp''[(c\text{-}C_5H_9)_7Si_8O_{13}]ZrCl_2$ (7a). To a toluene (30 mL) solution of $Cp''ZrCl_3$ (0.70 g, 1.72 mmol) was added **3** (1.90 g, 1.70 mmol) at room temperature. The white suspension that formed was stirred overnight. After the volatiles were removed under vacuum, the crude product was extracted (30 mL) with hexane. Evaporation of the solvent yielded a white foam. ^1H NMR spectroscopy revealed that a 2:1 mixture of $Cp''[(c\text{-}C_5H_9)_7Si_8O_{13}]ZrCl_2$ (**7a**) and $Cp''[(c\text{-}C_5H_9)_7Si_8O_{13}]_2ZrCl$ (**7b**) was formed. Due to their extreme solubility, separation of these products proved to be impossible. $Cp''[(c\text{-}C_5H_9)_7Si_8O_{13}]ZrCl_2$ (**7a**): ^1H NMR ($CDCl_3$, δ) 7.14 (t, 1H, $C_5H_3(SiMe_3)_2$, $^4J_{H-H} = 2$ Hz), 7.03 (d, 2H, $C_5H_3(SiMe_3)_2$, $^4J_{H-H} = 2$ Hz), 1.80 (m, 14H, CH_2-C_5H_9), 1.56 (m, 42H, CH_2-C_5H_9), 1.18 (m, 7H, CH-C_5H_9), 0.39 (s, 18H, $C_5H_3(Si(CH_3)_3)_2$); $^{13}C\{^1H\}$ NMR ($CDCl_3$, δ) 135.24 ($C_5H_3(SiMe_3)_2$), 130.09 ($C_5H_3(SiMe_3)_2$), 126.17 ($C_5H_3(SiMe_3)_2$), 27.32 (CH_2-C_5H_9), 27.26 (CH_2-C_5H_9), 27.01 (CH_2-C_5H_9), 22.13 (CH-C_5H_9), −0.49 ($C_5H_3(Si(CH_3)_3)_2$); ^{29}Si NMR (THF, δ) −7.36, −66.68, −66.84, −111.40 (2:3:4:1).

$Cp''[(c\text{-}C_5H_9)_7Si_8O_{13}]_2ZrCl$ (7b). Using the same procedures as for **7a**, starting with $Cp''ZrCl_3$ (0.77 g, 1.89 mmol) and **3** (4.24 g, 3.78 mmol), **7b** was obtained as an off-white foam (2.90 g, 1.34 mmol, 71%). ^1H NMR ($CDCl_3$, δ): 7.13 (t, $C_5H_3(SiMe_3)_2$, $^4J_{H-H} = 2$ Hz), 6.95 (d, $C_5H_3(SiMe_3)_2$, $^4J_{H-H} = 2$ Hz), 1.80 (m, 14H, CH_2-C_5H_9), 1.56 (m, 42H, CH_2-C_5H_9), 0.95 (m, 7H, CH-C_5H_9), 0.36 (s, 18H, $C_5H_3(Si(CH_3)_3)_2$). $^{13}C\{^1H\}$ NMR ($CDCl_3$, δ): 132.15 ($C_5H_3(SiMe_3)_2$), 124.80 ($C_5H_3(SiMe_3)_2$), 27.32, 27.27, 27.04 (CH_2-C_5H_9), 22.25, 22.19, 22.12 (1:3:3, CH-C_5H_9), −0.44 ($C_5H_3(Si(CH_3)_3)_2$). ^{29}Si NMR (toluene, δ): −7.85, −65.88, −66.42, −109.74 (1:3:4:1). Anal. Calcd for $C_{81}H_{147}ClO_{26}Si_{18}Zr$: C, 44.85; H, 6.83; Zr, 4.21. Found: C, 44.47; H, 6.93; Zr, 4.09.

---

[35] Abbenhuis, H. C. L.; Burrows, A. D.; Kooijman, H.; Lutz, M.; Palmer, M. T.; van Santen, R. A.; Spek, A. L. *Chem. Commun.* **1998**, 2627.

[36] (a) Winter, C. H.; Zhou, X.-X.; Dobbs, D. A.; Heeg, M. J. *Oganometallics* **1991**, *10*, 210. (b) Lancaster, S. J.; Robinson, O. B.; Bochmann, M.; Coles, S. J.; Hursthouse, M. B. *Organometallics* **1995**, *14*, 2456.

Cp″[Ph_3SiO]$TiCl_2$ (8a). At room temperature, a solution of Cp″$TiCl_3$ (4.9 g, 13.6 mmol) in toluene (35 mL) was added to a toluene (20 mL) solution of Ph_3SiOTl (6.5 g, 13.6 mmol). Immediately a white salt precipitated. After the mixture was stirred for 24 h, the toluene was evaporated and the residue was dried thoroughly. The crude product was dissolved in hexane (15 mL), and after filtration the clear orange to yellow filtrate was concentrated until crystallization started. Repeated crystallization (2×) at −30 °C yielded **8a** (6.0 g, 9.9 mmol, 73%) as an orange microcrystalline solid. ^1H NMR ($CDCl_3$, δ): 7.80 (d, 6H, C_6H_5), 7.48 (m, 9H, C_6H_5), 7.23 (s, 1H, $C_5H_3(SiMe_3)_2$), 6.84 (s, 2H, $C_5H_3(SiMe_3)_2$), 0.24 (s, 18H, $C_5H_3(Si(CH_3)_3)_2$). ^{13}C NMR ($CDCl_3$, δ): 141.8 (s, *ipso*-$C_5H_3(SiMe_3)_2$), 136.3 (d, C_6H_5, $^1J_{C-H} = 159$ Hz), 135.0 (s, *ipso*-C_6H_5), 134.1 (d, $C_5H_3(SiMe_3)_2$, $^1J_{C-H} = 172$ Hz), 131.0 (d, C_6H_5, $^1J_{C-H} = 160$ Hz), 129.6 (d, $C_5H_3(SiMe_3)_2$, $^1J_{C-H} = 174$ Hz), 128.6 (d, C_6H_5, $^1J_{C-H} = 160$ Hz), 0.2 (q, $C_5H_3(Si(CH_3)_3)_2$, $^1J_{C-H} = 119$ Hz). ^{29}Si NMR (toluene, δ): −6.3 ($C_5H_3(SiMe_3)_2$), −9.2 (Ph_3SiO) (2:1). Anal. Calcd for $C_{29}H_{36}Cl_2OSi_3Ti$: C,57.70; H, 6.01. Found: C, 57.49; H, 6.04.

Cp″[Ph_3SiO]$_2$TiCl (8b). The same procedures as for **8a** were used. Starting from Cp″$TiCl_3$ (1.0 g, 2.7 mmol) and Ph_3SiOTl (2.5 g, 5.2 mmol), gave **8b** (1.6 g, 1.9 mmol, 70%) as large rod-shaped yellow crystals. ^1H NMR ($CDCl_3$, δ): 7.68 (d, 12H, C_6H_5), 7.42 (m, 6H, C_6H_5), 7.31 (m, 12H, C_6H_5), 6.70 (s, 1H, $C_5H_3(SiMe_3)_2$), 6.58 (s, 2H, $C_5H_3(SiMe_3)_2$), 0.03 (s, 18H, $C_5H_3(Si(CH_3)_3)_2$). ^{13}C NMR ($CDCl_3$, δ): 137.0 (s, *ipso*-$C_5H_3(SiMe_3)_2$), 136.4 (d, C_6H_5, $^1J_{C-H} = 159$ Hz), 136.1 (s, *ipso*-C_6H_5), 130.8 (d, C_6H_5, $^1J_{C-H} = 151$ Hz), 130.9 (d, $C_5H_3(SiMe_3)_2$, $^1J_{C-H} = 170$ Hz), 128.3 (d, C_6H_5, $^1J_{C-H} = 159$ Hz), 0.3 (q, $C_5H_3(Si(CH_3)_3)_2$, $^1J_{C-H} = 121$ Hz). ^{29}Si NMR (toluene, δ): −7.3 ($C_5H_3(SiMe_3)_2$), −12.6 (Ph_3SiO) (1:1). Anal. Calcd for $C_{47}H_{51}ClO_2Si_4Ti(C_6H_{14})_{0.5}$: C, 67.73; H, 6.59. Found: C, 67.78; H, 6.63.

Cp″[Ph_3SiO]$_2$ZrCl (9). To a toluene (30 mL) solution of Ph_3SiOTl (2.0 g, 4.2 mmol) was added solid Cp″$ZrCl_3$ (0.8 g, 2.0 mmol) at room temperature. After the mixture was stirred for 24 h, the toluene was removed under vacuum and the residue was dried thoroughly. The crude product was dissolved in hexane (15 mL), filtered, and concentrated until crystallization started. Slow crystallization at room temperature afforded **9** (0.8 g, 0.9 mmol 45%) as long white needles, suitable for an X-ray crystal structure. ^1H NMR ($CDCl_3$, δ): 7.57 (d, 12H, C_6H_5, $^3J_{H-H} = 7.3$ Hz), 7.35 (t, 6H, C_6H_5, $^3J_{H-H} = 7.4$ Hz), 7.25 (t, 12H, C_6H_5, $^3J_{H-H} = 7.5$ Hz), 6.64 (t, 1H, $C_5H_3(SiMe_3)_2$, $^4J_{H-H} = 1.9$ Hz), 6.56 (d, 2H, $C_5H_3(SiMe_3)_2$, $^4J_{H-H} = 1.9$ Hz), 0.00 (s, 18H, $C_5H_3(Si(CH_3)_3)_2$). ^{13}C NMR ($CDCl_3$, δ): 135.7 (s, *ipso*-C_6H_5), 135.3 (d, C_6H_5, $^1J_{C-H} = 158$ Hz), 132.4 (s, *ipso*-$C_5H_3(SiMe_3)_2$), 129.8 (d, C_6H_5, $^1J_{C-H} = 159$ Hz), 128.1 (d, $C_5H_3(Si(CH_3)_3)_2$, $^1J_{C-H} = 168$ Hz), 127.9 (d, C_6H_5, $^1J_{C-H} = 159$ Hz), 125.1 (d, $C_5H_3(SiMe_3)_2$, $^1J_{C-H} = 170$ Hz), −0.4 (q, $C_5H_3(Si(CH_3)_3)_2$, $^1J_{C-H} = 119$ Hz). ^{29}Si NMR (toluene, δ): −8.5 ($C_5H_3(SiMe_3)_2$), −16.5 (Ph_3SiO) (1:1). The crystalline product gradually lost hexane from the lattice, preventing a reliable elemental analysis.

Cp″[(*c*-C_5H_9)$_7Si_8O_{13}$]Ti(CH_2Ph)$_2$ (10a). To a hexane (25 mL) solution of Cp″$Ti(CH_2Ph)_3$ (1.21 g, 2.28 mmol) was added solid **2** (2.10 g, 2.29 mmol) at 0 °C, and the mixture was warmed to room temperature. After the mixture was stirred for 2 h, traces of insoluble impurities were filtered off and the dark red solution was concentrated to approximately 5 mL. Slow crystallization at −30 °C afforded **10a** as a red microcrystalline material (2.00 g, 1.48 mmol, 64%). ^1H NMR (benzene-d_6, δ): 7.36 (m, 4H, *m*-C_6H_5), 7.28 (d, 4H, *o*-C_6H_5, $^3J_{H-H} = 7$ Hz), 7.00 (t, 2H, *p*-C_6H_5, $^3J_{H-H} = 7$ Hz), 6.89 (s, 1H, $C_5H_3(SiMe_3)_2$), 6.25 (s, 2H, $C_5H_3(SiMe_3)_2$), 3.48 (d, 2H, CH_2Ph, $^2J_{H-H} = 10$ Hz), 2.16 (d, 2H, CH_2Ph, $^2J_{H-H} = 10$ Hz), 1.97 (m, 14H, CH_2-C_5H_9), 1.75 (m, 28H, CH_2-C_5H_9), 1.58 (m, 14H, CH_2-C_5H_9), 1.26 (m, 7H, CH-C_5H_9), 0.37 (s, 18H, $Si(CH_3)_3$). ^{13}C NMR (benzene-d_6, δ): 149.04 (s, *ipso*-C_6H_5), 133.62 (s, $C_5H_3(SiMe_3)_2$), 129.55 (d, $C_5H_3(SiMe_3)_2$, $^1J_{C-H} = 159$ Hz), 128.53 (d, C_6H_5, $^1J_{C-H} = 158$ Hz), 127.75 (d, C_6H_5, $^1J_{C-H} = 158$ Hz), 126.16 (d, C_6H_5, $^1J_{C-H} = 157$ Hz), 123.03 (d, $C_5H_3(SiMe_3)_2$, $^1J_{C-H} = 158$ Hz), 86.82 (t, CH_2Ph, $^1J_{C-H} = 127$ Hz), 27.90 (t, CH_2-C_5H_9, $^1J_{C-H} = 130$ Hz), 27.50 (t, CH_2-C_5H_9, $^1J_{C-H} = 130$ Hz), 22.78 (d, CH-C_5H_9, $^1J_{C-H} = 119$ Hz), 0.14 (q, $Si(CH_3)_3$, $^1J_{C-H} = 120$ Hz). ^{29}Si NMR (toluene, δ): −7.98, −66.22, −66.70, −111.53 (2:3:4:1). Anal. Calcd for $C_{60}H_{98}O_{13}Si_{10}Ti$: C, 53.14; H, 7.28; Ti, 3.53. Found: C, 52.81; H, 7.19; Ti, 3.47.

Cp″[(*c*-C_5H_9)$_7Si_8O_{13}$]$TiMe_2$ (10b). Using the same procedure as for **10a**, starting with Cp″$TiMe_3$ (1.04 g, 3.44 mmol) and **2** (3.09 g, 3.37 mmol), afforded **10b** (2.10 g, 1.74 mmol, 51%) as a yellow crystalline material. ^1H NMR (benzene-d_6, δ): 7.17 (s, 1H, $C_5H_3(SiMe_3)_2$), 6.63 (s, 2H, $C_5H_3(SiMe_3)_2$), 1.68 (m, 56 H, CH_2-C_5H_9), 1.30 (m, 7H, CH-C_5H_9), 1.01 (s, 6H, CH_3), 0.24 (18H, $Si(CH_3)_3$). ^{13}C NMR (benzene-d_6, δ): 131.16 (s, $C_5H_3(SiMe_3)_2$), 124.71 (d, $C_5H_3(SiMe_3)_2$, $^1J_{C-H} = 163$ Hz), 123.22 (d, $C_5H_3(SiMe_3)_2$, $^1J_{C-H} = 164$ Hz), 56.56 (q, CH_3, $^1J_{C-H} = 123$ Hz), 27.94, 27.85, 27.50 (t, CH_2-C_5H_9, $^1J_{C-H} = 130$ Hz), 22.88, 22.77 (d, CH-C_5H_9, $^1J_{C-H} = 122$ Hz), −0.23 (q, $Si(CH_3)_3$, $^1J_{C-H} = 120$ Hz). ^{29}Si NMR (toluene, δ): −8.35, −66.26, −66.65, −111.06 (2:3:4:1). Anal. Calcd for $C_{48}H_{90}O_{13}Si_{10}Ti$: C, 47.88; H, 7.53; Ti, 3.98. Found: C, 47.63; H, 7.49; Ti, 3.67.

Cp″[Ph_3SiO]Ti(CH_2Ph)$_2$ (11a). At −80 °C, a toluene (20 mL) solution of Ph_3SiOH (1.2 g, 4.3 mmol) was added to a stirred solution of Cp″$Ti(CH_2Ph)_3$ (2.2 g, 4.1 mmol) in toluene (10 mL). After the addition, the mixture was slowly warmed to room temperature and the toluene was removed under vacuum, leaving a red oily residue. After the crude product was stripped with hexane (2 × 10 mL), it was dissolved in hexane (50 mL) and filtered hot. Slow cooling to 4 °C for crystallization afforded **11a** as large block-shaped crystals (2.0 g, 2.8 mmol, 68%). Concentration and cooling to −30 °C of the mother liquor yielded a second crop of **11a** as small red crystals (0.2 g, 0.3 mmol, 7%). ^1H NMR (benzene-d_6, δ): 7.59 (m, 6H, C_6H_5), 7.07 (m, 9H, C_6H_5), 6.92 (t, 4H, $C_6H_5CH_2$, $^3J_{H-H} = 7.4$ Hz), 6.73 (t, 6H, $C_6H_5CH_2$, $^3J_{H-H} = 7.4$ Hz), 6.69 (t, 1H, $C_5H_3(SiMe_3)_2$, $^4J_{H-H} = 1.8$ Hz), 6.15 (d, 2H, $C_5H_3(SiMe_3)_2$, $^4J_{H-H} = 1.8$ Hz), 3.16 (d, 2H, CH_2Ph, $^2J_{H-H} = 9.9$ Hz), 2.22 (d, 2H, CH_2Ph, $^2J = 9.9$ Hz), 0.40 (s, 18H, $C_5H_3(Si(CH_3)_3)_2$). ^{13}C NMR (benzene-d_6, δ): 149.9 (s, *ipso*-C_6H_5), 136.4 (s, *ipso*-C_6H_5), 136.4 (d, C_6H_5, $^1J_{C-H} = 156$ Hz), 133.7 (s, *ipso*-$C_5H_3(SiMe_3)_2$), 131.0 (d, $C_5H_3(SiMe_3)_2$, $^1J_{C-H} = 170$ Hz), 130.3 (d, C_6H_5, $^1J_{C-H} = 166$ Hz), 128.6 (d, C_6H_5, $^1J_{C-H} = 158$ Hz), 128.2 (d, C_6H_5, $^1J_{C-H} = 157$ Hz), 127.3 (d, C_6H_5, $^1J_{C-H} = 145$ Hz), 126.0 (d, $C_5H_3(SiMe_3)_2$, $^1J_{C-H} = 171$ Hz), 122.9 (d, C_6H_5, $^1J_{C-H} = 163$ Hz), 86.1 (t, CH_2Ph, $^1J_{C-H} = 125$ Hz), 0.3 (q, $C_5H_3(Si(CH_3)_3)_2$, $^1J_{C-H} = 120$ Hz). ^{29}Si NMR (toluene, δ): −8.1 ($C_5H_3(SiMe_3)_2$), −13.8 (Ph_3SiO) (2:1). Anal. Calcd for $C_{43}H_{50}OSi_3Ti$: C, 72.23; H, 7.05. Found: C, 72.26; H, 6.83.

Cp″[Ph_3SiO]Ti(CH_3)$_2$ (11b). The same procedure as for **11a**, staring with Cp″$TiMe_3$ (1.1 g, 3.6 mmol) and Ph_3SiOH (1.0 g, 3.6 mmol), afforded **11b** (1.7 g, 2.9 mmol, 81%) as a yellow solid after removal of the hexane and thorough drying. ^1H NMR (benzene-d_6, δ): 8.15 (m, 6H, C_6H_5), 7.45 (m, 9H, C_6H_5), 6.78 (s, 1H, $C_5H_3(SiMe_3)_2$), 6.72 (s, 2H, $C_5H_3(SiMe_3)_2$), 1.10 (s, 6H, CH_3), 0.24 (s, 18H, $C_5H_3(Si(CH_3)_3)_2$). ^{13}C NMR (benzene-d_6, δ): 136.7 (s, *ipso*-C_6H_5), 135.8 (d, C_6H_5, $^1J_{C-H} = 158$ Hz), 131.1 (s, *ipso*-$C_5H_3(SiMe_3)_2$), 130.0 (d, C_6H_5, $^1J_{C-H} = 160$ Hz), 128.0 (d, C_6H_5, $^1J_{C-H} = 157$ Hz), 124.3 (d, $C_5H_3(SiMe_3)_2$, $^1J = 170$ Hz), 122.9 (d, $C_5H_3(SiMe_3)_2$, $^1J = 170$ Hz), 55.8 (q, CH_3, $^1J_{C-H} = 128$ Hz), 0.3 (q, $C_5H_3(Si(CH_3)_3)_2$, $^1J = 116$ Hz). ^{29}Si NMR (toluene, δ): −8.5 ($C_5H_3(SiMe_3)_2$), −16.4 (Ph_3SiO) (2:1). Anal. Calcd for $C_{31}H_{42}OSi_3Ti$: C, 66.15; H, 7.52. Found: C, 65.54; H, 7.63.

Cp″[Ph_3SiO]Zr(CH_2Ph)$_2$ (12a). At −80 °C, solid Ph_3SiOH (1.2 g, 4.3 mmol) was added to a stirred solution of Cp″$Zr(CH_2Ph)_3$ (2.44 g, 4.25 mmol) in toluene (50 mL). The mixture was slowly warmed to room temperature, after which the solvent was removed under vacuum. To remove traces of toluene, the sticky solid was dissolved in hexane (10 mL) and subsequently dried under vacuum. This procedure was repeated (2×) until a nonsticky solid was obtained. Crystallization from hexane (20 mL) at −30 °C yielded **12a** as yellow crystals (1.8 g, 2.37 mmol, 56%). ^{1}H NMR (benzene-d_6, δ): 7.77 (m, 6H, C_6H_5), 7.30 (m, 9H, C_6H_5), 7.09 (m, 4H, $C_6H_5CH_2$), 6.97 (m, 6H, $C_6H_5CH_2$), 6.90 (s, 1H, $C_5H_3(SiMe_3)_2$), 6.45 (s, 2H, C_5H_3-$(SiMe_3)_2$), 2.50 (d, 2H, CH_2Ph, $^2J_{H-H} = 11.0$ Hz), 2.10 (d, 2H, CH_2Ph, $^2J_{H-H} = 11.0$ Hz), 0.20 (s, 18H, $C_5H_3(Si(CH_3)_3)_2$). ^{13}C NMR (benzene-d_6, δ): 145.4 (s, *ipso*-C_6H_5), 136.8 (s, *ipso*-C_6H_5), 136.2 (d, C_6H_5, $^1J_{C-H} = 158$ Hz), 130.4 (d, C_6H_5, $^1J_{C-H} = 159$ Hz), 130.2 (s, *ipso*-$C_5H_3(SiMe_3)_2$), 129.7 (d, C_6H_5, $^1J_{C-H} = 158$ Hz), 128.3 (d, C_6H_5, $^1J_{C-H} = 157$ Hz), 128.2 (d, C_6H_5, $^1J_{C-H} = 145$ Hz), 127.4 (d, $C_5H_3(SiMe_3)_2$, $^1J_{C-H} = 171$ Hz), 123.4 (d, C_6H_5, $^1J_{C-H} = 156$ Hz), 123.2 (d, $C_5H_3(SiMe_3)_2$, $^1J_{C-H} = 177$ Hz), 63.1 (t, CH_2Ph, $^1J_{C-H} = 124$ Hz), 0.5 (q, $C_5H_3(Si(CH_3)_3)_2$, $^1J_{C-H} = 119$ Hz). ^{29}Si NMR (toluene, δ): −9.0 ($C_5H_3(SiMe_3)_2$), −17.4 (Ph_3SiO) (2:1). Anal. Calcd. for $C_{43}H_{50}OSi_3Zr$: C, 68.10; H, 6.65. Found: C, 67.81; H, 6.73.

Cp″[Ph_3SiO]$_2$Zr(CH_2Ph) (12b). Using the same procedure as for **12a** and starting with Ph_3SiOH (0.9 g, 3.3 mmol) and Cp″Zr(CH_2Ph)$_3$ (0.9 g, 1.6 mmol) yielded **12b** (0.8 g, 0.8 mmol, 52%) as an off-white crystalline solid. ^{1}H NMR (benzene-d_6, δ): 7.78 (d, 12H, C_6H_5, $^3J_{H-H} = 6.8$ Hz), 7.21 (m, 18H, C_6H_5, $^3J_{H-H} = 6.8$ Hz), 7.04−6.83 (m, 5H, C_6H_5), 6.79 (t, 1H, C_5H_3-$(SiMe_3)_2$, $^4J_{H-H} = 1.9$ Hz), 6.74 (d, 2H, $C_5H_3(SiMe_3)_2$, $^4J_{H-H} = 1.9$ Hz), 2.84 (s, 2H, CH_2Ph), 0.15 (s, 18H, $C_5H_3(Si(CH_3)_3)_2$). ^{13}C NMR (benzene-d_6, δ): 148.3 (s, *ipso*-C_6H_5), 137.0 (s, *ipso*-C_6H_5), 136.2 (d, C_6H_5, $^1J_{C-H} = 158$ Hz), 130.3 (d, C_6H_5, $^1J_{C-H} = 159$ Hz), 130.0 (s, *ipso*-$C_5H_3(SiMe_3)_2$), 129.5 (d, CH_2Ph, $^1J_{-H} = 158$ Hz), 128.4 (d, C_6H_5, $^1J_{C-H} = 163$ Hz), 128.2 (d, C_6H_5, $^1J_{C-H} = 145$ Hz), 126.9 (d, $C_5H_3(SiMe_3)_2$, $^1J_{C-H} = 168$ Hz), 124.7 (d, $C_5H_3(SiMe_3)_2$, $^1J_{C-H} = 170$ Hz), 122.4 (d, C_6H_5, $^1J_{C-H} = 161$ Hz), 59.3 (t, CH_2Ph, $^1J_{C-H} = 119$ Hz), 0.4 (q, $C_5H_3(Si(CH_3)_3)_2$, $^1J_{C-H} = 119$ Hz). ^{29}Si NMR (toluene, δ): −9.1 ($C_5H_3(SiMe_3)_2$), −17.6 (Ph_3SiO) (1:1). Anal. Calcd for $C_{54}H_{58}O_2Si_2Zr$: C, 68.81; H, 6.20. Found: C, 68.08; H, 6.26.

[(*c*-C_5H_9)$_7$$Si_7O_{12}$]TiCp″ (13). To a deep yellow solution of Cp″$TiCl_3$ (1.64 g, 4.51 mmol) in CH_2Cl_2 (40 mL) was added (*c*-C_5H_9)$_7$$Si_7O_9(OH)_3$ (3.98 g, 4.55 mmol). The color of the suspension changed to light yellow immediately following the addition of pyridine (1.5 mL, 18.6 mmol). After the mixture was warmed to reflux for 5 min, the solvent was evaporated and the product was extracted with hexanes (30 mL). The filtrate was evaporated to dryness, and the product was washed with acetone (4 × 10 mL). Recrystallization of the crude product from a toluene/acetonitrile mixture at room temperature yielded **13** as pale yellow crystals (2.67 g, 2.36 mmol, 52%). ^{1}H NMR ($CDCl_3$, δ): 6.87 (s, 1H, $C_5H_3(SiMe_3)_2$), 6.79 (s, 2H, $C_5H_3(SiMe_3)_2$), 1.79 (m, 14H, CH_2-C_5H_9), 1.56 (m, 42H, CH_2-C_5H_9), 0.98 (m, 7H, CH-C_5H_9), 0.36 (s, 18H, C_5H_3-$(Si(CH_3)_3)_2$). ^{13}C NMR ($CDCl_3$, δ): 132.91 (d, CH-$C_5H_3(SiMe_3)_2$, $^1J_{C-H} = 170$ Hz), 130.28 (s, C_{ipso}-$C_5H_3(SiMe_3)_2$), 125.45 (d, CH-$C_5H_3(SiMe_3)_2$, $^1J_{C-H} = 167$ Hz), 27.89 (t, CH_2-C_5H_9, $^1J_{C-H} = 130$ Hz), 27.36 (t, CH_2-C_5H_9, $^1J_{C-H} = 131$ Hz), 27.07 (t, CH_2-C_5H_9, $^1J_{C-H} = 129$ Hz), 22.80 (d, CH-C_5H_9, $^1J_{C-H} = 118$ Hz), 22.29 (d, CH-C_5H_9, $^1J_{C-H} = 117$ Hz), −0.27 (q, $C_5H_3(Si(CH_3)_3)_2$, $^1J_{C-H} = 120$ Hz). ^{29}Si{^{1}H} NMR (toluene, δ): −8.17 ($SiMe_3$), −64.43, −66.60, −67.64 (2:3:1:3). Anal. Calcd for $C_{46}H_{84}O_{12}$-Si_9Ti: C, 48.90; H, 7.49; Ti, 4.24. Found: C, 48.87; H, 7.55; Ti, 4.20.

[(*c*-C_5H_9)$_7$$Si_7O_{12}$]ZrCp″ (14). To a frozen (liquid N_2) solution of Cp″$ZrMe_3$ (0.56 g, 1.62 mmol) in toluene (20 mL) was added (*c*-C_5H_9)$_7$$Si_7O_9(OH)_3$ (1.42 g, 1.62 mmol). The mixture was slowly warmed to room temperature. The resulting pale yellow solution was stirred for an additional 1 h, after which the solvent was evaporated, leaving a crystalline solid. Recrystallization from CH_2Cl_2 at −30 °C yielded **14** as colorless crystals (1.17 g, 1.00 mmol, 62%). ^{1}H NMR ($CDCl_3$, δ): 6.86 (t, 1H, $C_5H_3(SiMe_3)_2$, $^4J_{H-H} = 2$ Hz), 6.82 (d, 2H, $C_5H_3(SiMe_3)_2$, $^4J_{H-H} = 2$ Hz), 1.76 (m, 14H, CH_2-C_5H_9), 1.54 (m, 42H, CH_2-C_5H_9), 0.96 (m, 7H, CH-C_5H_9), 0.36 (18H, $C_5H_3(Si(CH_3)_3)_2$). ^{13}C NMR ($CDCl_3$, δ): 129.94 (s, C_{ipso}-$C_5H_3(SiMe_3)_2$), 128.82 (d, $C_5H_3(SiMe_3)_2$, $^1J_{C-H} = 170$ Hz), 123.34 (d, $C_5H_3(SiMe_3)_2$, $^1J_{C-H} = 168$ Hz), 27.78 (t, CH_2-C_5H_9, $^1J_{C-H} = 131$ Hz), 27.34 (t, CH_2-C_5H_9, $^1J_{C-H} = 130$ Hz), 27.11 (t, CH_2-C_5H_9, $^1J_{C-H} = 129$ Hz), 22.78 (d, CH-C_5H_9, $^1J_{C-H} = 119$ Hz), 22.41 (d, CH-C_5H_9, $^1J_{C-H} = 117$ Hz), 22.34 (d, CH-C_5H_9, $^1J_{C-H} = 117$ Hz), −0.34 (q, C_5H_3-$(Si(CH_3)_3)_2$, $^1J_{C-H} = 119$ Hz). ^{29}Si NMR (toluene, δ): −9.17 ($SiMe_3$), −64.32, −66.53, −68.29 (1:3:1:3). Anal. Calcd for $C_{46}H_{84}O_{12}Si_9Zr$: C, 47.10; H, 7.22; Zr, 7.78. Found: C, 46.85; H, 7.25; Zr, 7.74.

X-ray Diffraction Studies of 9 and 11a. Suitable crystals were measured at 130 K with graphite-monochromated Mo Kα radiation on an Enraf-Nonius CAD-4F diffractometer equipped with a low-temperature unit.[37] Precise lattice parameters and their standard deviations and orientation matrix were derived from the angular settings of 22 reflections (**9**, $18.24° < \theta < 20.08°$; **11a**, $16.52° < \theta < 20.34°$) in four alternative settings.[38] The unit cell was identified as rhombohedral (space group $R\bar{3}$ (H, obv.)) for **9** and triclinic (space group $P\bar{1}$) for **11a**.[39] Intensity data were corrected for Lorentz and polarization effects and scale variation and reduced to F_o^2.[40] The structures were solved by Patterson methods, and extension of the model was accomplished by direct methods applied to difference structure factors using the program DIRDIF.[41] The positional and anisotropic thermal displacement parameters for the non-hydrogen atoms were refined on F^2 with full-matrix least-squares procedures minimizing the function $Q = \sum_h[w(|F_o^2 - kF_c^2|)^2]$, where $w = 1/[\sigma^2(F_o^2) + (aP)^2 + bP]$ and $P = [\max(F_o^2,0) + 2F_c^2]/3$. F_o and F_c are the observed and calculated structure factor amplitudes, respectively; a and b were refined. Reflections were stated observed if they satisfied the $F^2 > 0$ criterion of observability. For **9**, refinement was complicated by distortion of the cyclopentadienyl trimethylsilyl groups. For both Si1−C6⋯C8 and Si2−C9⋯C11, two positions were found with major site occupancy factors of 0.53(7) and 0.55(3), respectively. Probably due to the presence of the highly distorted trimethylsilyl groups and to a large extent disappeared solvent (hexane) molecules from the holes in the lattice, peaks not exceeding 1.5 e/Å^3 in the last residual Fourier maps were found, but their geometry could not be rationalized. Neutral atom scattering factors and anomalous dispersion corrections were taken from ref 42. All calculations were carried out on a HP9000/735 computer at the University of Groningen with the program packages SHELXL,[43] PLATON,[44] and ORTEP.[45]

pK_a Measurements. The pK_a measurements were carried out using the overlapping indicator method as described by Bordwell et al.[29] 9-Cyanofluorene (pK_a(DMSO) = 8.3) and 9-(methoxycarbonyl)fluorene (pK_a(DMSO) = 10.4) were the indicators used. Lithium salts of the indicators were prepared, isolated, and recrystallized before use. The pK_a values of the indicators are determined in DMSO.[29] Due to the very low solubility of silsesquioxanes in DMSO, THF was used as the

---

(37) Van Bolhuis, F. *J. Appl. Crystallogr.* **1971**, *4*, 263.

(38) De Boer, J. L.; Duisenberg, A. J. M. *Acta Crystallogr.* **1984**, *A40*, C410.

(39) No higher metric lattice symmetry or extra metric symmetry elements were found: (a) Spek, A. L. *J. Appl. Crystallogr.* **1988**, *21*, 578. (b) Le Page, Y. *J. Appl. Crystallogr.* **1987**, *20*, 264. (c) Le Page, Y. *J. Appl. Crystallogr.* **1988**, *21*, 983.

(40) Spek, A. L. HELENA Program for Data Reduction; University of Utrecht, Utrecht, The Netherlands, 1993.

(41) Beurskens, P. T.; Beurskens, G.; Bosman, W. P.; de Gelder, R.; García-Granda, S.; Gould, R. O.; Israël, R.; Smits, J. M. M. The DIRDIF-97 Program System; Crystallography Laboratory, University of Nijmegen, Nijmegen, The Netherlands, 1992.

(42) *International Tables of Crystallography*; Wilson, A. J. C., Ed.; Kluwer Academic: Dordrecht, The Netherlands, 1992; Vol. C.

(43) Sheldrick, G. M. SHELX-97: Program for the Solution and Refinement of Crystal Structures; University of Göttingen, Göttingen, Germany, 1997.

(44) Spek, A. L. PLATON: Program for the Automated Analysis of Molecular Geometry; University of Utrecht, Utrecht, The Netherlands, 1996.

(45) Johnson, C. K. ORTEPII; Report ORNL-5138; Oak Ridge National Laboratory, Oak Ridge, TN, 1976.

solvent instead. pK_a values can differ dramatically, depending on the solvent used (e.g. PhOH: pK_a(H_2O) = 10.0, pK_a(DMSO) = 18.0),[29d] ion pairing, and chelate formation.[29e] Hence, the reported pK_a's are no absolute values but are solely qualitative values relative to the (arbitrary) indicator pK_a values.

DFT Computational Studies. Density functional theory (DFT) forms the basis of our calculations, as implemented by the Amsterdam density functional (ADF) code.[46] The exchange correlation functionals in the local-density approximation[47] were augmented by generalized gradient approximations to the exchange[48] and correlation.[49] All the corrections were applied self-consistently. We choose a double-ζ set of Slater type basis functions with polarization function for carbon, oxygen, and fluorine with frozen core of the 1s electrons. The same basiss, but with no frozen core and a 2p core, was used for hydrogen and silicon, respectively. The basis for titanium was triple-ζ with polarization function and a 2p frozen core. A quasi Newtonian approach[50] to geometry optimization is combined with the direct inversion in the iterative subspace method (DIIS).[51] Full geometry optimization has been used in all calculations in this work. The convergence criteria used in these calculations are 10^{-3} hartree for the energy, 5×10^{-3} hartree/Å for the gradients, and 5×10^{-3} Å for the Cartesian displacement. ADF code makes use of the natural symmetry properties of the different clusters. The silsesquioxanes were approximated by substituting the large cyclopentadienyl groups on the silicon atoms by hydrogens.

Ethylene Polymerization. Ethylene polymerization experiments were carried out in a 1.3 L stainless steel reactor equipped with a stationary steel stirrer. In a typical experiment, under nitrogen PMH (pentamethylheptane, 600 mL) was brought into the reactor. The contents were heated with stirring to the required temperature. Additionally, a constant ethylene pressure was maintained. A toluene (10 mL) solution of the cocatalyst (MAO or $B(C_6F_5)_3$) was syringed into a 100 mL catalyst-dosing vessel containing PMH (25 mL). Subsequently, the solution was transferred into the reactor. After 15 min, the desired amount of catalyst precursor was introduced into the reactor in the same way, after which the catalyst-dosing vessel was washed automatically with PMH (2 × 50 mL). The polymerization reactions were carried out under isothermal conditions and constant ethene pressure. At the end of the reaction, the reaction mixture was collected and quenched with 20 mL of methanol. Antioxidant (Irganox 1076) was added to stabilize the polymer. The polymer was dried under vacuum at 70 °C for 24 h and analyzed by GPC.

1-Hexene Polymerization. In a glovebox, **10a** and **11a** (20 μmol) and $B(C_6F_5)_3$ (0.2 mmol) were dissolved in neat 1-hexene (10 mL). The homogeneous solution was stirred for 16 h at 25 °C. The polymer obtained was washed with ethanol and H_2O to remove the catalyst. Thorough drying yielded the polymer as a viscous, sticky oil. The polymer was identified by ^1H and ^{13}C NMR and characterized by GPC analysis.

Acknowledgment. This work was financially supported by DSM Research BV, which is gratefully acknowledged. We also thank Dr. S. J. R. Creve (DSM Research) for calculating the cone angles. R.J.H. thanks the German Science Foundation (DFG) and the National Computing Facilities Foundation (NCF) for financial support.

Supporting Information Available: Tables of atomic coordinates, thermal displacement parameters, bond lengths, bond angles, and torsion angles for **9** and **11a**. This material is available free of charge via the Internet at http://pubs.acs.org.

OM9904495

---

(46) ADF 2.3.0; Theoretical Chemistry, Vrije Universiteit Amsterdam, Amsterdam, The Netherlands: (a) Baerends, E. J.; Ellis, D. E.; Ros, P. *Chem. Phys.* **1973**, *2*, 41. (b) te Velde, G.; Baerends, E. J. *J. Comput. Phys.* **1992**, *99*, 84.

(47) Vosko, S. H.; Wilk, L.; Nusair, N. *Can. J. Phys.* **1980**, *58*, 1200.

(48) Becke, A. D. *Phys. Rev. A* **1988**, *38*, 3098.

(49) Perdew, J. P. *Phys. Rev. B* **1986**, *33*, 8822.

(50) Fan, L.; Ziegler, T. *J. Chem. Phys.* **1991**, *95*, 7401.

(51) Fisher, T. H.; Almlöf, J. *J. Chem. Phys.* **1992**, *96*, 9768.